รายงานวิจัยฉบับสมบูรณ์

โครงการ

อิทธิพลของวิธีการอบแห้งแบบต่าง ๆ ที่มีต่อคุณภาพของกล้วย

โดย

รศ.ดร. สมเกียรติ ปรัชญาวรากร

มิถุนายน พ.ศ. 2551

สัญญาเลขที่ RMU 4880002

รายงานวิจัยฉบับสมบูรณ์

โครงการ อิทธิพลของวิธีการอบแห้งแบบต่าง ๆ ที่มีต่อคุณภาพของกล้วย

มหาวิทยาลัยเทคโนโลยีพระจอมเกล้าธนบุรี

สนับสนุนโดยสำนักงานคณะกรรมการการอุดมศึกษา
และสำนักงานกองทุนสนับสนุนการวิจัย

(ความเห็นในรายงานนี้เป็นของผู้วิจัย สกอ. และ สกว. ไม่จำเป็นต้องเห็นด้วยเสมอไป)

บทคัดย่อ

น้ำมันที่คงเหลืออยู่ในผลิตภัณฑ์กล้วยอบกรอบมีอายุในการเก็บรักษาสั้นเนื่องจากมีกลิ่นหืนซึ่งเกิดจากปฏิกิริยาออกซิเดชันของไขมัน เพื่อเลี่ยงปัญหาดังกล่าวในงานวิจัยนี้จึงศึกษาวิธีการผลิตกล้วยกรอบด้วยวิธีการอบแห้งแบบต่างๆ การทำโฟมกล้วย นอกจากนี้ยังศึกษาถึงผลของการพรีทรีทเมนต์กล้วยก่อนการอบแห้งเพื่อป้องกันการเกิดปฏิกิริยาสีน้ำตาลต่อคุณภาพของกล้วยกรอบ

การอบแห้งด้วยอุณหภูมิสูงในช่วงระหว่าง 110 ถึง 140°Cเพียงอย่างเดียวเพื่อลดความชื้นจากความชื้นร้อยละ 250 มาตรฐานแห้ง เหลือความชื้นต่ำกว่าร้อยละ 3 มาตรฐานแห้ง ซึ่งเป็นความชื้นที่ต้องการสำหรับของขบเคี้ยวทั่วไป พบว่าผลิตภัณฑ์ที่ได้มีสีน้ำตาลค่อนข้างเข้มแม้ว่ากล้วยจะผ่านการพรีทรีทเมนต์ก่อนการอบแห้งด้วยกรดเอสคอร์บิค โซเดียมเมตาไบซัลไฟต์ และการลวก กล้วยแผ่นที่ผ่านการลวกจะมีความแข็งน้อยขณะที่มีการหดตัวมาก สีของผลิตภัณฑ์และคุณภาพทางด้านความกรอบ เช่นจำนวนของยอด และความชันเริ่มต้น ดีขึ้นเมื่อผ่านการอบแห้งแบบหลายขั้นตอน ซึ่งประกอบไปด้วย การอบแห้งด้วยลมร้อนที่อุณหภูมิต่ำ เพื่อลดความชื้นของผลิตภัณฑ์ลงมาระดับหนึ่ง จากนั้นนำไปผ่านกระบวนการพัฟฟิงด้วยไอน้ำร้อนยวดยิ่งที่อุณหภูมิสูงประมาณ 180°C เป็นระยะเวลาสั้น ๆ และในขั้นตอนสุดท้ายเป็นการอบแห้งที่อุณหภูมิต่ำเพื่อลดความชื้นให้ได้ความชื้นตามที่ต้องการ เมื่อเปรียบเทียบการอบแห้งการอบแห้งวิธีนี้กับการอบแห้งแบบสูญญากาศร่วมกับรังสีอินฟราเรด (vacuum FIR)และการอบแห้งแบบแช่เยือกแข็ง (FD) พบว่าผลิตภัณฑ์ที่ผ่านการอบแห้งแบบหลายขั้นตอนมีความกรอบมากกว่าและหดตัวน้อยกว่าการอบแห้งแบบ vacuum FIR แต่สีที่ได้ค่อนข้างมีสีน้ำตาลเข้มกว่าโดยผลิตภัณฑ์ที่ได้จัดอยู่ในกลุ่มสี Greyed-orange 163C กล้วยที่ผ่านการอบแห้งแบบ FD มีสีเหลืองอ่อน และไม่กรอบ สารประกอบที่ระเหยง่ายสูญเสียไปมากสำหรับการอบแห้งแบบหลายขั้นตอนและ vacuum FIR ขณะที่การอบแห้งด้วย FD สามารถรักษาปริมาณสารประกอบที่ระเหยง่ายไว้ได้

นอกจากวิธีการอบแห้งดังกล่าวข้างต้นแล้ว การทำโฟมกล้วยก่อนนำมาอบแห้งสามารถผลิตกล้วยกรอบได้เช่นกัน แผ่นโฟมกล้วยหลังการอบแห้งมีความแข็งน้อยกว่ากล้วยที่ไม่ผ่านการทำโฟมและระดับความกรอบและความแข็งขึ้นอยู่กับความหนาแน่นของแผ่นโฟมกล้วยเริ่มต้น อุณหภูมิในการอบแห้งซึ่งอยู่ในช่วงระหว่าง 60 ถึง 80°C ไม่มีผลต่อคุณภาพในด้านต่างๆ ของแผ่นโฟมกล้วย อย่างไรก็ตามแผ่นโฟมกล้วยที่ได้ค่อนข้างมีการหดตัวสูงถึงร้อยละ 50 ทั้งนี้เนื่องจากโฟมที่ก่อขึ้นมีการยุบตัวลงขณะอบแห้ง ในการผลิตแผ่นโฟมกล้วยกรอบควรใช้ความหนาแน่นของโฟมกล้วยเริ่มต้นประมาณ 0.5 g/cm^3 และผ่านการอบแห้งที่ 80°C ที่เงื่อนไขดังกล่าวนี้ค่าความแข็งและความกรอบที่ได้ใกล้เคียงกับขนมปังกรอบที่ผลิตขายเป็นเชิงพาณิชย์ (Hi Crack ™)

จากผลงานวิจัยที่กล่าวมาทั้งหมดข้างต้นสามารถผลิตบัณฑิตในระดับดุษฎีบัณฑิตเป็นจำนวน 1 ท่าน ระดับมหาบัณฑิตเป็นจำนวน 5 ท่าน และระดับบัณฑิตศึกษา 9 ท่าน พร้อมกับมีผลงานวิจัยที่ตีพิมพ์ในวารสารระดับนานาชาติเป็นจำนวน 4 เรื่อง ในวารสารระดับชาติ 1 เรื่อง ในการประชุมวิชาการระดับนานาชาติ 2 เรื่องและในการประชุมวิชาการระดับประเทศ 8 เรื่อง

ABSTRACT

The oil content remaining in deep-fried banana causes a short shelf life of the product due to lipid oxidation leading to rancidity. To alleviate this problem, this research was therefore to study the method to produce the crispy banana by using foaming technique and different drying techniques viz. hot air drying, vacuum far infrared drying (vacuum FIR), freeze drying (FD) and multistage drying. Furthermore, the pretreatment methods in order to prevent the browning reactions were also studied and considered their effect on the quality of crispy banana.

The banana slices after decreasing moisture content below 4% d.b., which is normally required for snack, using air temperatures of 110 to 140°C had intense brown although the samples before drying was pretreated with anti browning reagents viz. ascorbic acid, sodium metabisulphide and blanching. The banana sample pretreated by blanching had lower hardness but highest shrinkage as compared to other reagents. The finished product color and texture property in terms of number of peaks and initial slope (stiffness) from the force deformation curve can be significantly improved when the banana slices was processed with multistage drying. In multistage drying, the samples were dried with hot air at low temperature in order to reduce moisture to certain level. They were then dried or puffed with superheated steam at 180°C for a very short period of time and dried again to the desired moisture content using low-temperature drying. The finished product quality obtained by the multistage drying when compared to the above-mentioned drying methods was very different. The banana dried by multistage drying was crispier and lower shrinkage than the vacuum FIR-dried banana, but the product color was relatively browner, corresponding to the color group of grayed-orange 163C. However, the volatile compounds of finished product as measured by GC-MS device lost in a large quantity for the samples from the vacuum FIR and multistage drying, but could be maintained almost the same as those of fresh banana for the FD-dried product. However, the FD-dried product was not crispy.

In addition to the above drying methods, foaming banana before drying can produce the crisp banana. The fresh egg white was used as a foaming agent. The hardness of dried foamed banana was generally significantly smaller as compared to that of the finished product obtained from the above drying methods. The degree of crispness, as characterized by the number of peaks and initial slopes, and hardness of dried banana foam was depended on the banana foam density before drying. The drying temperature in the range of 60 to 80°C insignificantly affected the quality parameters such as texture and color. Due to instability of egg white foaming agent, the produced banana foam was collapsed during drying and consequently, the sample was shrunk by approximately 50% of the thickness at beginning of drying. To produce the crisp banana foam, it recommended to prepare the banana foam density of 0.5 g/cm^3 and dry it at 80°C. The finished product obtained at the recommended condition had hardness and texture property similar to the Hi Crack ^{TM} commercial cracker.

One PhD student, 5 Master students and 9 undergraduate students were the output of this research work, along with 4 papers published in the international journal, one paper in local journal, 2 papers in the international conferences and 8 papers in the national conferences.

ปัญหาที่ทำการวิจัย และความสำคัญของปัญหา

กล้วยเป็นพืชล้มลุกที่สามารถออกผลได้ตลอดทั้งปี และเป็นที่นิยมปลูกกันอย่างแพร่หลาย ทำให้ผลผลิตที่ออกสู่ท้องตลาดมีมากเกินความต้องการของผู้บริโภค และการเก็บรักษากล้วยในลักษณะของสดเป็นสิ่งไม่ง่ายนัก เนื่องกล้วยจะมีการเปลี่ยนแปลงอย่างรวดเร็วในลักษณะของเนื้อสัมผัสและสีหลังจากที่กล้วยสุก กล่าวคือ กล้วยเขียวจะมีลักษณะของเนื้อกล้วยที่แข็ง จะเปลี่ยนเป็นกล้วยที่มีสีเหลือง พร้อมกับเนื้อที่มีลักษณะนิ่มและนุ่มขึ้น เมื่ออยู่ในช่วงที่ระดับความสุกที่เหมาะสม และเนื้อเยื่อจะมีลักษณะที่ยุ่ยมากเมื่อกล้วยสุกงอมมากเกินไป เนื่องจากคุณภาพของกล้วยลดลงและเน่าเสียอย่างรวดเร็วหลังจากที่มีการเก็บเกี่ยว การนำกล้วยที่สุกแล้วมาผ่านกระบวนการอบแห้งเป็นทางเลือกหนึ่งที่สามารถลดปริมาณการสูญเสีย และสามารถนำไปใช้ประโยชน์ต่อได้ นอกจากประโยชน์ดังกล่าวแล้วการอบแห้งยังเป็นการเพิ่มมูลค่าของผลิตภัณฑ์ เพื่อให้บรรลุวัตถุประสงค์ดังกล่าวการจัดการอบแห้งกล้วยเป็นไปไม่ง่ายนัก เนื่องจากกล้วยเป็นพืชที่มีปริมาณน้ำตาลค่อนข้างสูง จากรายงานการวิจัยที่ผ่านมาพบว่าการใช้อุณหภูมิสูงในการอบแห้งเป็นระยะเวลานานสำหรับผลิตภัณฑ์ที่มีน้ำตาลเป็นองค์ประกอบเป็นสาเหตุที่ทำให้เกิดการสูญเสีย กลิ่น สี คุณค่าทางโภชนาการ และ สมบัติการคืนตัวของผลิตภัณฑ์หลังการอบแห้ง

กล้วยแผ่นเป็นผลิตภัณฑ์ที่สามารถนำไปใช้ประโยชน์ได้มากมาย เช่น เป็นอาหารว่าง เป็นส่วนผสมในเมล็ดธัญพืชสำหรับทานเป็นอาหารเช้า (breakfast cereals) นอกจากนี้อาจนำกล้วยแผ่นไปผ่านกระบวนการแปรรูปอื่นๆ เพื่อให้ได้ผลิตภัณฑ์สุดท้ายตามที่ต้องการ เช่น เคลือบด้วยสารให้ความหวาน หรือการทอดในน้ำมัน คุณภาพของกล้วยแผ่นหลังการอบแห้งจึงมีลักษณะที่แตกต่างกันทั้งนี้ขึ้นอยู่กับลักษณะของผลิตภัณฑ์สุดท้ายที่ต้องการ อย่างไรก็ตามในงานวิจัยนี้มีวัตถุประสงค์ที่จะนำกล้วยมาผลิตเป็นอาหารว่าง หรือ ใช้เป็นส่วนผสมในเมล็ดธัญพืชสำหรับทานเป็นอาหารเช้า ลักษณะของผลิตภัณฑ์ดังกล่าวควรมีลักษณะของความกรอบและหวาน ลักษณะของเนื้อกล้วยไม่ควรที่จะนิ่มง่ายเกินไปหลังจากที่สัมผัสกับของเหลว จากลักษณะของสมบัติดังกล่าวในทางปฏิบัติทำได้โดยการทอดภายใต้สภาวะสุญญากาศ แม้ว่าเทคนิคดังกล่าวจะประสบความสำเร็จในระดับหนึ่ง แต่ข้อปัญหาที่เกิดขึ้นตามมา คือ มีปริมาณน้ำมันยังคงเหลืออยู่ในผลิตภัณฑ์ ดังรายงานการวิจัยสำหรับการทอดผลิตภัณฑ์ชนิดต่าง ๆ นอกจากนี้การที่มีปริมาณน้ำมันคงค้างภายในผลิตภัณฑ์อาจทำให้เกิดปฏิกิริยาออกซิเดชันทำให้เกิด กลิ่นหืนและไม่เป็นที่นิยมสำหรับผู้บริโภคที่ใส่ใจในสุขภาพ

การไล่ความชื้นออกจากวัสดุสามารถกระทำได้ด้วยกันหลายวิธี เช่น การนำความร้อน การพาความร้อน และการแผ่รังสีความร้อน แต่ละรูปแบบของการให้ความร้อนทำให้เกิดการเคลื่อนที่ของความชื้นที่แตกต่างกัน การเคลื่อนที่ของความชื้นอาจอยู่ในรูปของการแพร่ หรือเกิดขึ้นโดยอาศัยแรงคาปิลลารี ผลจากรูปแบบของการเคลื่อนที่ของความชื้นและวิธีการให้ความร้อนที่

แตกต่างกัน ทำให้ได้ลักษณะทางกายภาพของผลิตภัณฑ์แตกต่างกัน การใช้อากาศร้อนในการอบแห้งมักพบว่าโครงสร้างของวัสดุมักจะเกิดชั้นแข็งที่บริเวณผิวรอบนอกของวัสดุ และวัสดุมีการหดตัว การหดตัวของวัสดุจะมากหรือน้อยขึ้นอยู่กับอุณหภูมิที่ใช้ในการอบแห้งและปริมาณความชื้นที่สูญเสียไป และผลจากการหดตัวของวัสดุส่งผลต่อคุณภาพของผลิตภัณฑ์ เช่น สูญเสียสมบัติในการคืนรูปของวัสดุ อย่างไรก็ตามเมื่อทำการอบแห้งโดยใช้ ปั๊มความร้อนร่วมกับการใช้อากาศร้อน พบว่า สมบัติในการคืนรูปดีขึ้นเมื่อเทียบกับการใช้อากาศร้อนเพียงอย่างเดียว สำหรับการให้ความร้อนโดยการแผ่รังสีนั้น รังสีที่ใช้ในปัจจุบันมีด้วยกัน 2 ชนิด คือ ไมโครเวฟ และอินฟราเรด ความยาวคลื่นที่ใช้ในการอบแห้งโดยทั่วไปอยู่ในช่วงระหว่าง 2.5 ถึง 30 μm สำหรับอินฟราเรด และในช่วงความยาวคลื่น 100 μm ถึง 1 m สำหรับไมโครเวฟ การให้ความร้อนด้วยวิธีการ แผ่รังสีนั้นสามารถลดการเกิดชั้นแข็งที่บริเวณผิวรอบนอกซึ่งส่งผลให้อัตราการอบแห้งเร็วขึ้นและคุณภาพของผลิตภัณฑ์ดีขึ้น ทั้งนี้เนื่องจากเป็นการให้ความร้อนภายในวัสดุ

จากรายงานวิจัยที่ผ่านมาจะเห็นว่า ส่วนใหญ่เน้นศึกษาผลกระทบของการอบแห้งที่มีต่อลักษณะทางกายภาพของผลิตภัณฑ์หลังอบแห้ง แต่การศึกษาเกี่ยวกับสารระเหยง่ายที่มีอยู่ในผลิตภัณฑ์ซึ่งมีส่วนสำคัญในการยอมรับคุณภาพของอาหารแต่ยังไม่แพร่หลายนัก แน่นอนที่สุดวิธีที่สามารถรักษากลิ่นของผลิตภัณฑ์ให้คงอยู่นั้นควรใช้อุณหภูมิและความดันต่ำในการอบแห้ง ซึ่งภายใต้เงื่อนไขดังกล่าวไม่อาจที่จะหลีกเลี่ยงได้ด้วยการใช้เทคนิคของการแช่เยือกแข็ง (freeze drying) อย่างไรก็ตามด้วยวิธีของการแช่เยือกแข็งนี้ มีค่าใช้จ่ายในการอบแห้งค่อนข้างสูงมากและใช้เวลาในการอบแห้งนาน ด้วยสาเหตุดังกล่าวในงานวิจัยนี้จึงเป็นการศึกษาวิธีการอบแห้งด้วยเทคนิคต่าง ๆ ที่มีผลต่อคุณภาพของกล้วยแผ่น โดยมีความคาดหวังเพื่อให้ได้คุณภาพของผลิตภัณฑ์ใกล้เคียงกับคุณภาพของผลิตภัณฑ์ที่ได้จาการอบแบบแช่เยือกแข็งแต่มีค่าใช้จ่ายในการอบแห้งต่ำกว่า

นอกจากการศึกษาวิธีการอบแห้งที่มีต่อคุณภาพของกล้วยแล้ว ขั้นตอนการเตรียมก่อนการอบแห้งก็มีส่วนสำคัญเช่นเดียวกัน ทั้งนี้เนื่องจากในกล้วย ผลไม้และผักต่าง ๆ มีเอนไซม์โพลีฟีนอลออกซิเดซ(Polyphenol oxidase) โดยส่วนใหญ่เอนไซม์เหล่านี้มักอยู่ที่บริเวณชั้นรอบ ๆ นอกของเซลล์ ดังนั้นโอกาสที่เอนไซม์เหล่านี้จะไปสัมผัสกับออกซิเจนจึงเกิดขึ้นได้ง่าย ส่งผลให้เอนไซม์มีความว่องไวและเป็นตัวเร่งปฏิกิริยาระหว่างสารประกอบพวกฟีนอลกับออกซิเจนทำให้เกิดเป็นสีน้ำตาล (Enzymatic browning reaction) ขึ้น ซึ่งสีที่เกิดขึ้นนี้ส่วนใหญ่เป็นผลมาจากขั้นของการลอกเปลือกของผลไม้และการเก็บรักษา วิธีที่นิยมปฏิบัติกันทั่วไปสำหรับป้องกันปฏิกิริยาสีน้ำตาลที่มีเอนไซม์เกี่ยวข้อง คือ นำผลิตภัณฑ์ก่อนการอบแห้งจุ่มลงในสารละลายที่มีซัลเฟอร์เป็นองค์ประกอบ เช่น โซเดียม เมตาไบซัลไฟต์ (sodium metabisulfide) เป็นต้น ทั้งนี้เนื่องจากเป็นวิธีที่ให้ประสิทธิภาพสูงและเป็นสารเคมีที่มีราคาไม่แพง อย่างไรก็ตามการจุ่มผักหรือผลไม้ลงในสารละลายนี้ ทำให้ความชื้นของผลิตภัณฑ์ก่อนนำมาอบแห้งมีความชื้นสูงขึ้นและเป็นผลทำให้มีความสิ้นเปลือง

พลังงานสูงขึ้นและเพิ่มเวลาในการอบแห้งนานขึ้น นอกจากนี้การใช้สารละลายที่มีซัลเฟอร์เป็นองค์ประกอบยังส่งผลต่อสุขภาพสำหรับบุคคลบางกลุ่มที่ไวต่อสิ่งกระตุ้นดังกล่าว

ดังนั้นในงานวิจัยนี้จึงเกี่ยวข้องกับการศึกษาการเตรียมตัวอย่างกล้วยก่อนการอบแห้ง รวมทั้งศึกษาถึงวิธีการอบแห้งโดยใช้เทคนิคต่าง ๆ เพื่อให้ได้คุณภาพของผลิตภัณฑ์ที่ดี สำหรับรายละเอียดของผลการศึกษาที่ได้จากงานวิจัยนี้สามารถอ่านได้จากบทความต่างๆ ที่ได้แนบมากับรายงานฉบับนี้

Available online at www.sciencedirect.com
ScienceDirect
Journal of Food Engineering 85 (2008) 509–517
JOURNAL OF FOOD ENGINEERING
www.elsevier.com/locate/jfoodeng

Drying kinetics and quality attributes of low-fat banana slices dried at high temperature

Somkiat Prachayawarakorn [a,*], Warunee Tia [b], Napaporn Plyto [b], Somchart Soponronnarit [b]

[a] *Faculty of Engineering, King Mongkut's University of Technology, Thonburi, 126 Pracha u-tid, Bangkok 10140, Thailand*
[b] *School of Energy, Environment and Materials, King Mongkut's University of Technology, Thonburi, 126 Pracha u-tid, Bangkok 10140, Thailand*

Received 13 December 2006; received in revised form 8 August 2007; accepted 10 August 2007
Available online 23 August 2007

Abstract

High temperature drying may give rise to hydrostatic pressure gradients of moisture inside the dried sample and subsequently leads to large voids, resulting in crispy product. In this study, the drying characteristics as well as various quality attributes, namely, colors, shrinkage and textural property of banana slices dried at high temperatures (110–140 °C) in a tray dryer were explored. Banana slices were dried from the initial moisture content of 250–300% dry basis to the required final moisture content of 4% dry basis. The analysis of the drying rate evolution revealed three drying regimes, i.e., warming-up and two falling rate periods. The effective diffusion coefficient of banana was found to increase with a decrease of the moisture content until a certain moisture content after which the diffusivity decreased. In terms of quality, the large pore assembly was produced at higher temperature of 120 °C as observed from SEM micrographs. The drying temperature also significantly affected the colors, shrinkage and texture of bananas.
© 2007 Elsevier Ltd. All rights reserved.

Keywords: Colors; Effective diffusivity; Snack; Texture

1. Introduction

Bananas are a favourite fruit widely grown in the areas of tropical and subtropical climates. After harvesting, the quality of bananas deteriorates rapidly. Drying is largely utilized to stabilize the product by reducing its moisture content. In addition to preservation, drying can also create new range of products and this indeed adds value to fresh bananas. Banana chips are one of the value-added products from fresh bananas. Banana chips can be consumed as a snack or used as an ingredient in breakfast cereal. To produce banana chips, thin-sliced bananas are normally fried with vegetable oil. However, the obtained product generally contains high oil content and cannot be kept for an extended period of time due to possible lipid oxidation leading to rancidity. To alleviate this problem, drying can be employed instead to produce banana chips. To obtain chips with desired texture (crispness), high temperature drying is needed to generate internal pressure gradients.

Migration of moisture and transfer of heat induce stresses inside food materials, which consequently lead to many physical changes such as cell wall collapse and shrinkage (Lozano, Rotstein, & Urbricain, 1983; Panyawong & Devahastin, 2007; Tsami & Katsioti, 2000). Such deformations are the determinant of textural properties in foods. Several studies have reported that higher drying rates, obtained by higher drying temperatures, result in higher degrees of deformation of food products (Li, Seyed-Yagoobi, Moreira, & Yamsaengsung, 1999; Markowski, Cenkowski, Hatcher, Dexter, & Edwards, 2003). Hofsetz and Lopes (2005) indeed reported that crispy bananas obtained by the combination of high temperature and short time drying stage required less force to break and exhibited many fracture points from the plot of force–deformation curve as drying temperature and time increased.

In addition to the above physical changes, other organoleptic properties including colors are altered when foods

* Corresponding author. Tel.: +662 470 9221; fax: +662 428 3534.
E-mail address: somkiat.pra@kmutt.ac.th (S. Prachayawarakorn).

0260-8774/$ - see front matter © 2007 Elsevier Ltd. All rights reserved.
doi:10.1016/j.jfoodeng.2007.08.011

Nomenclature

D	effective moisture diffusion coefficient, m^2/s	m_{ph}	mass of cylindrical tube with *n*-heptene, g
L	thickness of material, m	m_{phs}	mass of cylindrical tube including *n*-heptene and sample, g
M	moisture content, dry basis decimal	m_s	mass of sample, g
M_{in}	initial moisture content, dry basis decimal	t	drying time, s
M_{eq}	equilibrium moisture content, dry basis decimal	V	volume of sample, cm^3
M_s	moisture content at the surface of banana slice, dry basis decimal	*Greek Letter*	
MR	moisture ratio, $\frac{M(t)-M_{eq}}{M_{in}-M_{eq}}$, dimensionless	ρ_h	density of *n*-heptane, g/cm^3
m_p	mass of cylindrical tube, g		

are exposed to thermal treatment. The changes in colors of foods are the results of the browning reactions and pigment degradation (Barreiro, Milano, & Sandoval, 1997; Lopez et al., 1997; Maskan, 2001). The color changes, more or less, depend on the reducing sugar content, the temperature and the exposure time (Feng & Tang, 1998; Ibarz, Pagán, & Garza, 1999; Krokida, Tsami, & Urbricain, 1998; Márquez & AnWón, 1986). Spectrophotometer and tristimulus colorimeter are frequently used to examine the colors of the products. The latter method was used to determine the color changes of banana slices in the present work.

In this work, drying kinetics, color changes, morphology and textural properties of banana slices were studied. The Fick's second law of diffusion coupled with an optimization technique was also utilized to determine the effective diffusion coefficient of bananas undergoing high temperature drying.

2. Materials and methods

2.1. Experimental set-up

Banana slices were dried using a tray dryer consisting of a 0.3 m × 0.3 m × 0.1 m drying chamber, a 13.5 kW electrical heater and a backward curved blade centrifugal fan driven by a 2.2 kW motor as schematically shown in Fig. 1. The samples were placed on a stainless steel tray. The bottom surfaces of the samples, which were contacted with the tray, were not exposed to hot air. The desired air speed was controlled by a frequency inverter, which governed the rotation speed of the motor.

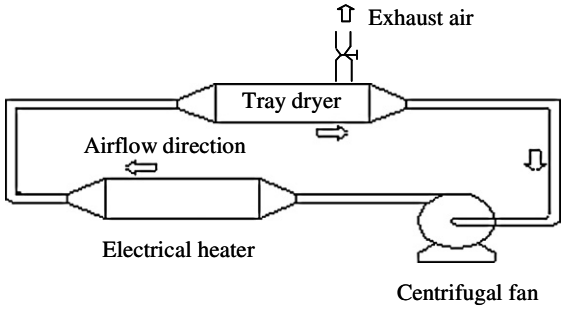

Fig. 1. Schematic diagram of tray drying system.

2.2. Material preparation

Gros Michel bananas were purchased from a local supermarket at the dark green stage and were allowed to ripen at room temperature. The fresh bananas contained soluble solids content of approximately 23–25° Brix as measured by a refractometer and had the yellow and green tip, corresponding to the color index no. 5 (Anon, 1972). The initial moisture content of bananas ranged between 250% and 300% dry basis. After peeling bananas were sliced to 3 mm thickness using a cutting machine.

2.3. Drying of banana slices

Before starting of each drying experiment, the drying system was warmed up until the required temperature was attained. Drying of banana slices was performed at the temperatures of 110, 120, 130 and 140 °C and at the superficial air velocity of 0.9 m/s. Inlet air temperature was controlled by a PID type controller with an accuracy of ±1 °C. The samples were taken out from the dryer to determine their moisture content at every 5 min using an electronic balance with a precision of ±0.01 g. At the end of each experiment, the moisture content of the samples was determined by drying them in an oven at 103 °C for 3 h. The drying experiments were performed in triplicate.

2.4. Color measurement

The colors of banana slices were measured both before drying and at different predetermined periods by a Minolta CR-300 colorimeter. Because the colors of the dried samples were not uniform throughout their surface, being rather brown near the central area and yellow near the periphery, the samples were ground before each color measurement. Each data point presented was obtained from the measurement of 10 samples. The colors were expressed as *L*-value (brightness/darkness), *a*-value (redness/greenness) and *b*-value (yellowness/blueness).

2.5. Texture measurement

Dried banana slices at moisture content of 4% dry basis were kept in sealed plastic bags at room temperature for two days prior to texture measurement. Textural attributes of banana were measured using a texture analyzer TAXT2i fitted with a 5-N load cell. The samples were fractured with a 2-mm cylindrical probe using a test speed of 1 mm/s. The probe moved down vertically and crossed over the sample slice placed on the base. The maximum compression force and the stiffness (initial slope) in the force–deformation curve of each sample were considered as an indication of the hardness and crispness of the sample, respectively. Ten measurements were performed on the samples obtained from each drying condition.

2.6. Microstructural evaluation

The morphology of fresh and dried bananas was characterized through the use of a scanning electron microscope [model JEOL 5800LV, Tokyo, Japan] at an accelerating voltage of 10 kV. Before scanning for the morphology of the fresh banana, the specimens were dehydrated in the ascending ethanol concentrations of 10%, 30%, 50%, 70%, 90% and 100%. The sample was then dried by the critical point method (Dinand, Chanzy, & Vignon, 1999; Silva & Luh, 1978) in a Tousimis Samdri b780 critical point dryer (Tousimis, Rockville, USA) operated with CO_2. For the dried samples, they were dipped into liquid N_2 for 5 s. Before photographing, the specimens was prepared and made into the dimensions of 5×5 mm^2 and then glued on the metal stub. The samples were then coated with gold (~20 nm thickness) and scanned and photographed.

2.7. Shrinkage measurement

Ten samples were used for each shrinkage measurement. Shrinkage was defined as the difference in volume of the original sample and that of the dried sample relative to that of the original volume:

$$\%\ \text{shrinkage} = \frac{V_i - V}{V_i} \times 100 \tag{1}$$

where V_i and V are the volume of the fresh sample and the volume of the dried sample, respectively. The volume of each sample was measured using *n*-heptane as the replacement liquid. Each sample was first weighted and placed in a cylindrical tube. The sample volume, V, was then calculated using the following equation:

$$V = \frac{[m_{ph} - m_p] - [m_{phs} - m_p - m_s]}{\rho_h} \tag{2}$$

where m_{ph} is the mass of the cylindrical tube with *n*-heptane, m_p is the mass of empty cylindrical tube, m_{phs} is the mass of the cylindrical tube with sample and *n*-heptane, m_s is the mass of the sample and ρ_h is the density of *n*-heptane. The average value of ten samples was reported. An error of the measurement was ±2.0% by volume.

2.8. Determination of moisture diffusivity of bananas

In this study, banana slices were assumed to have an infinite slab shape. Therefore, the moisture diffusion within each slice is described by the Fick's second law (Crank, 1975):

$$\frac{\partial M(x,t)}{\partial t} = \frac{\partial}{\partial x}\left(D(M)\frac{\partial M(x,t)}{\partial x}\right) \tag{3}$$

or

$$\frac{\partial M(x,t)}{\partial t} = D(M)\frac{\partial^2 M(x,t)}{\partial x^2} + \frac{\partial M(x,t)}{\partial x}\cdot\frac{\partial D(M)}{\partial x} \tag{4}$$

If the effective diffusion coefficient is constant, the last term on the right hand side of Eq. (4) needs not be considered. To calculate the moisture profiles inside each banana slice from Eq. (4), the initial and boundary conditions are required. In this work, it was assumed that the mass transfer resistance due to convection was negligible and the moisture diffusion occurred at an isothermal condition. During drying the evaporation of moisture occurred from the top surface, which was exposed to hot air, while no moisture evaporation took place at the bottom since the sample surface was covered with foil. The following initial and boundary conditions were then used:

$$M(x,t) = M_{in} \quad 0 \leqslant x \leqslant L \text{ at } t = 0 \tag{5}$$

$$M(L,t) = M_{eq} \quad x = L \text{ at } t > 0 \tag{6}$$

$$\text{and} \quad \frac{\partial M(x,t)}{\partial x} = 0 \quad x = 0 \text{ at } t > 0 \tag{7}$$

Eq. (4) was discretized using a forward time central space method (FTCS):

Internal node:

$$\frac{M_i^{t+1} - M_i^t}{\Delta t} = D_i\left(\frac{M_{i+1}^t - 2M_i^t + M_{i-1}^t}{\Delta x^2}\right) + \left(\frac{M_{i+1}^t - M_{i+1}^t}{2\Delta x}\right)\left(\frac{D_{i+1}^t - D_{i-1}^t}{2\Delta x}\right) \tag{8}$$

At the top surface:

$$M_s^t = M_{eq} \tag{9}$$

At the bottom:

$$\frac{M_0^{t+1} - M_0^t}{\Delta t} = 2D_0^t\left(\frac{M_{i+1}^t - M_i^t}{\Delta x^2}\right) \tag{10}$$

To estimate the effective moisture diffusivity as a function of moisture content, the optimization technique using simplex method was used. Before optimization, it was necessary to identify the equation, which could describe the

relationship between the moisture and the diffusivity. Several equations reported by Sano and Yamamoto (1990) and Yoshida, Imakoma, and Okazaki (1991) were first tested and the calculated results showed that those equations inadequately fitted with the experimental results as indicated by R^2 values which were less than 0.5.

Another empirical form which could suitably describe the relationship between the diffusion coefficient and the moisture content as well as the temperature is

$$D = A\exp\left(bM + cM^2 + dM^3 + eM^4 + \frac{H}{T}\right) \quad (11)$$

where A, b, c, d, e and H are the constant parameters obtained from the optimization. Eq. (11) was found to adequately describe the diffusion coefficients of porous food materials, e.g., biscuit, bread, muffin and cooked rice (Ramesh, 2003; Tong & Lund, 1990). In the calculation the sample was divided into 20 nodes and Δt of 0.1 s was used.

3. Results and discussion

3.1. Drying characteristic curves

Fig. 2 shows the semi-log scale plot of drying curves of banana slices at temperatures of 110, 120, 130 and 140 °C. These curves reveal that the decrease of moisture content with time is in a non-linear fashion, indicating that the moisture movement is controlled by diffusion and that diffusion is dependent on the moisture content of the samples.

Improvement of drying rates was rather different at different drying temperatures. As shown in Fig. 2, the moisture decrease was slightly faster at 120 °C than at 110 °C. However, when the drying temperature shifted from 120 to 130 °C, much larger difference in the moisture reduction rates was observed. The higher capability of removing moisture at temperatures higher than 120 °C can possibly be explained by a couple of reasons. Firstly, banana morphology was different; large pores inside banana were formed at temperature higher than 120 °C. These large pores facilitated the transport of moisture. The details of pore formation will be discussed later. The acceleration of the movement of water molecules at higher temperatures also took part in a more rapid decrease of the moisture content.

Fig. 3 presents the experimental drying rates of banana slices at different drying temperatures. Drying of banana slices exhibited three distinct drying periods, warming-up and two falling rate periods. In the warming-up period, the drying rates were almost constant as the moisture content of the sample reduced from the initial moisture content to approximately 220% dry basis. This drying period existed for a very short period of time, approximately 4–7 min depending on the drying temperature used.

In the latter drying periods, the drying rates decreased with a decrease in the moisture. During the first falling rate period, the drying rates decreased non-linearly with the moisture content until the moisture content reached approx. 80% dry basis as shown in Fig. 3. Then, the second falling rate started. The drying rates in the second falling rate period decreased linearly and more slowly than the first falling rate period.

Some early works relevant to banana drying have also reported three drying regimes although the drying conditions employed were different. Mowlah, Takano, Kamoi, and Obara (1983) and Jannot, Talla, Nganhou, and Puiggali (2004) found a warming up period followed by two falling rate periods. Sankat, Castaigne, and Maharaj (1996) observed the two falling rate periods when drying both fresh and osmotically-dehydrated banana slices. In their work, the critical moisture content, at which the decrease of the drying rate with the moisture content changed from the linear to non-linear fashion, was found at the moisture content around 100% dry basis which was relatively high compared with that observed in the present study (approx. 80% dry basis). The difference of the values of critical moisture content is possibly due to different moisture gradients and surface moistures, according to different drying conditions.

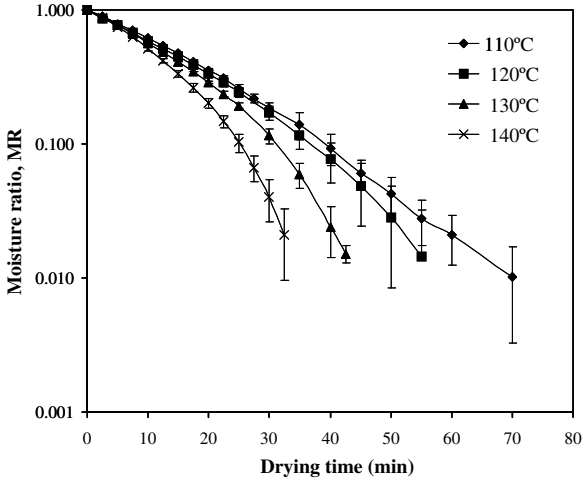

Fig. 2. Drying curves of banana slices at different temperatures.

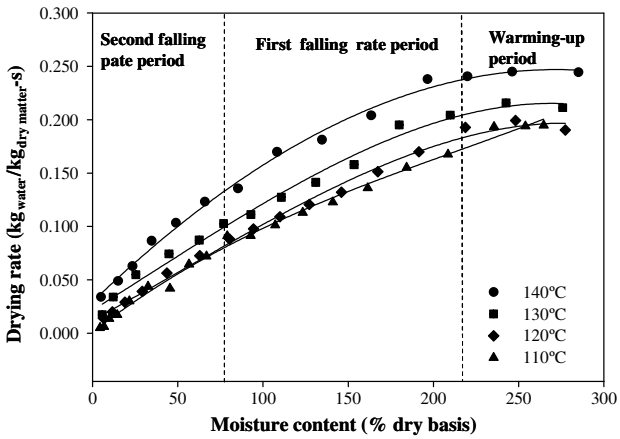

Fig. 3. Drying rates of banana slices at different temperatures.

As shown in Fig. 3, the drying rates of banana slices at the temperature of 120 °C are slightly higher than those at the temperature of 110 °C. Beyond 120 °C, the drying rates were greatly enhanced with increasing temperature throughout the entire range of moisture content.

3.2. Moisture diffusivity of bananas

Fig. 4 shows the dependence of effective diffusion coefficient on the moisture content and temperature. The effective diffusion coefficient increased with a decrease of the moisture content, then reached the maximum value at the range of the moisture content of 50–60% dry basis and eventually decreased with the moisture content. This trend of the change of moisture diffusivity with moisture content is similar to that reported in the case of drying porous granular Amioca (Karathanos, Villalobos, & Saravacos, 1990) and in the case of adsorption of water vapor by the dried biscuit (Guillard, Broyart, Guilbert, Bonazzi, & Gontard, 2004).

The trend of increasing moisture diffusivity noted in the present study is opposite to that reported in the literature, which shows the monotonic decrease of the moisture diffusivity as the moisture content decreases (Sankat et al., 1996). The different trends are possibly due to different drying conditions which may produce different mechanisms and morphologies of banana slices. The vapor diffusion of water is possibly the main mechanism of mass transfer in our work whereas liquid diffusion is dominant in low temperature drying ($T < 80$ °C). In addition, shrinkage of banana and the formation of pores facilitated the transport of moisture from the inside to the outside of the samples. At lower moisture contents of 60% dry basis, which was in the second falling rate period, the values of effective diffusion coefficient dropped sharply since water in the bananas was strongly bound on the sorption sites of the sample solid matrix.

The constant parameters in Eq. (11) obtained from the numerical method, together with R^2 value, are shown in Table 1. These constant parameters were reasonably used in the moisture range of 4–250% dry basis and the temperature range of 110–140 °C.

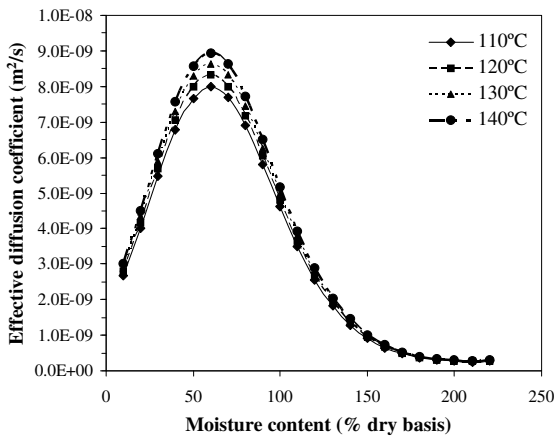

Fig. 4. Effective diffusion coefficients of banana slices at different temperatures.

Table 1
Constant parameters in Eq. (11) at drying temperatures

Constant parameters						R^2
A	b	c	d	e	H	
7.67×10^{-9}	5.53	−5.02	0.176	0.361	−595.43	0.954

3.3. Morphology of bananas

Fig. 5 shows the morphologies of banana slices dried at the temperatures of 110, 120, 130 and 140 °C. After drying morphologies of banana slices were noticeably different from that of the reference sample; the dried samples became porous whilst the morphology of the reference sample was relatively dense. The pore formation after drying is possibly due to the evolution of the water vapor inside the samples. Such change in turn led to the development of the internal pressure and breakage of the sample tissues, resulting in pore formation. These pores might affect not only the transport properties such as the diffusivities of gases and liquids in the samples, but also the crisp texture of the samples, which is essentially required for snack foods.

As shown in Fig. 5, the produced pores were irregular in shape and random in size. The pore development depended strongly on the drying temperature used. The highly porous banana slices were obtained when using the temperatures higher than 120 °C, with larger pore sizes of 100 μm. The dried banana slices became less porous at lower drying temperatures, particularly at temperature 110 °C.

3.4. Colors

Fig. 6 shows the evolution of color parameters with the drying time and temperature. When the drying time was longer, the colors of banana slices changed from slight yellow to brown, which corresponded to increase in the ΔL-values and Δa-values, presenting darker and redder of banana slices. On the other hand, the Δb-values exhibited oscillatory feature, increasing during an early period of drying until reaching the maximum values and then dropping to the lowest values before rising up again at the later period of drying. According the above changes, the L-values were the most sensitive color parameter during drying. This was followed by the a-values and the b-values, being the least sensitive color parameter. For example, ΔL-value, Δa-value and Δb-value of a dried banana slice were, respectively, 30, 16 and 4 at the drying temperature of 110 °C. Note that the L-, a- and b-values of fresh banana were 78 ± 2.2, -2.6 ± 0.4 and 27 ± 1.7, respectively.

The trends of the changes of L- and a-values with the drying time were similar to the color changes of kiwifruits

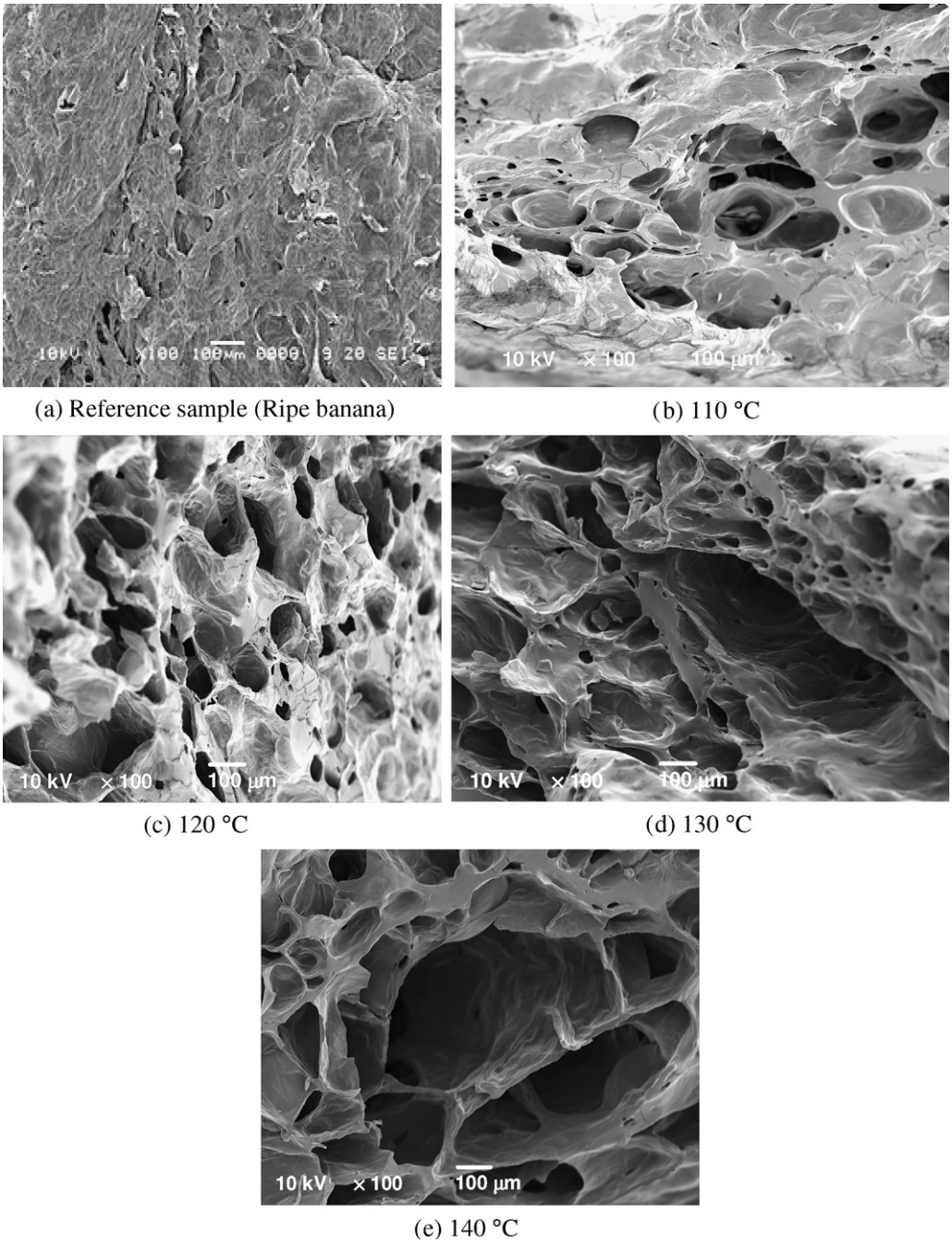

Fig. 5. Morphologies of banana slice after drying at different drying temperatures.

during microwave drying (Maskan, 2001). The reduced luminosity involves the destruction of thermolabile pigments, which consequently results in the formation of dark compounds (Barreiro et al., 1997). An increase of the *a*-value, on the other hand, may be due to the formation of brown pigments (Lopez et al., 1997; Maskan, 2000).

As shown in Fig. 6, the changes of *L*-, *a*- and *b*-values during the first 20 min of drying were only slightly different over the drying temperature range of 110–130 °C. This period of drying corresponded to higher moisture content than 100% dry basis, which covered the warming-up period and some parts of the first falling rate period. In this moisture range, the moisture content of banana slices was sufficiently high and the product temperature during drying might not be very different within the drying temperature range of 110–130 °C; this is because the heat transferring to bananas was mostly utilized for vaporizing moisture instead of heating the bananas. Accordingly, the rates of browning reactions were not very different amongst the high and low temperature drying. Hence, color differences were still small. At lower moisture content, corresponding to the second falling rate period where drying rates

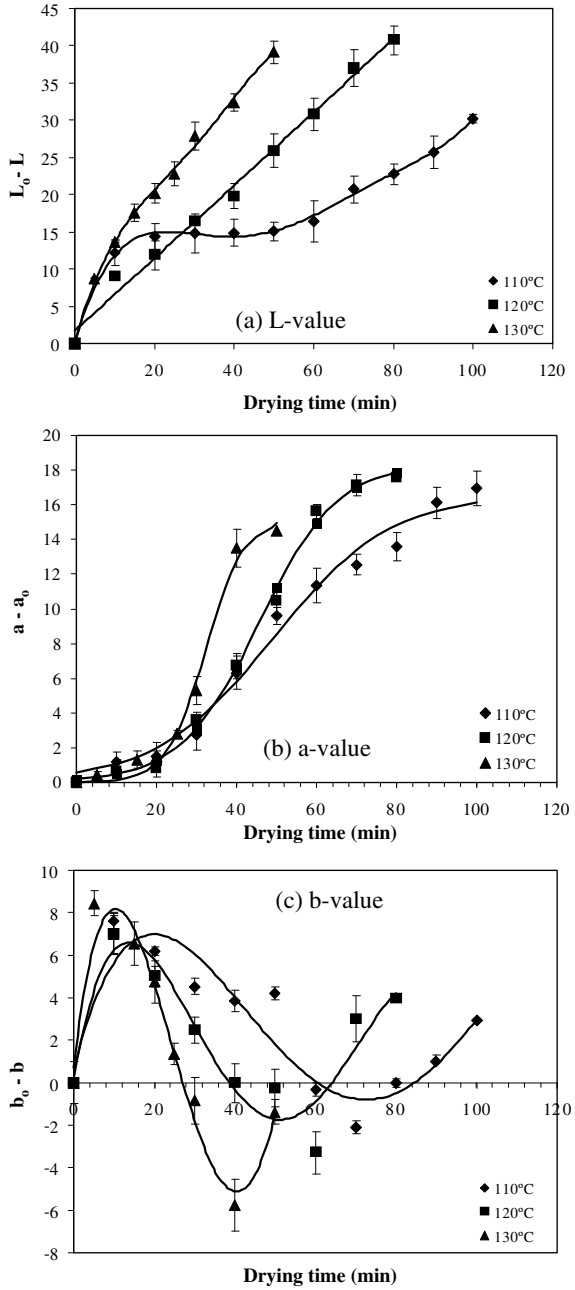

Fig. 6. Evolution of color parameters for banana slices with times and temperatures.

dropped rapidly (see Fig. 3), however, the color changes with time were rapid because the product temperature increased rapidly.

3.5. Shrinkage

Fig. 7 shows the shrinkage of dried banana slices. The initial thickness of bananas was 3 mm. When banana slices were exposed to heat, they shrunk. The shrinkage of bananas depended on the drying temperature used. A lesser extent of shrinkage was found at higher drying temperatures. The percentages of shrinkage for dried bananas were

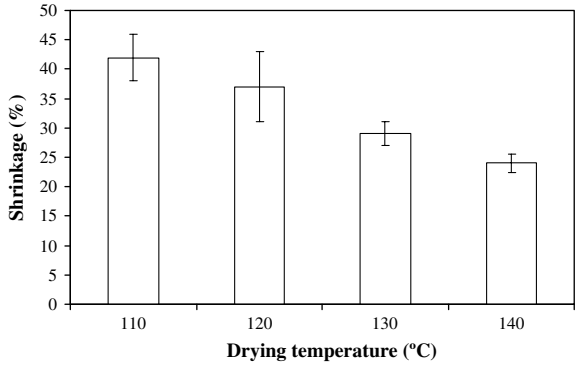

Fig. 7. Shrinkage of banana slices at different temperatures.

$42\% \pm 4$, $37\% \pm 6$, $29\% \pm 2$ and $24\% \pm 1.5$ when using the drying temperatures of 110, 120, 130 and 140 °C, respectively. The lower shrinkage of bananas at higher drying temperatures can be attributed to the lower moisture content of the external surfaces, which might induce a rubbery-glass transition and the resulting formation of rigid crust at the outer layer that helped fixing the size of samples (Mayor & Sereno, 2004). On the other hand, as drying proceeded, the internal tissues split and broke, rendering the large pore formation as previously shown in Fig. 5. Wang and Brennan (1995), Del Valle, Cuadros, and Aguilera (1998) and Li et al. (1999) also noted the formation of larger pore sizes at higher temperatures.

3.6. Textural properties

Fig. 8 shows the hardness of banana slices at the end of drying. The final moisture content of banana slices taken to examine the texture ranged between 3% and 5% dry basis. The values of hardness were between 6 and 10 N for banana slices dried in the temperature range of 110–140 °C. The statistical analysis using Duncan's test indicated the insignificant effect of the drying temperature on the hardness ($P > 0.05$).

However, the effect of temperature on the stiffness was significant as shown in Fig. 9, revealing that high values of stiffness were obtained at higher drying temperatures.

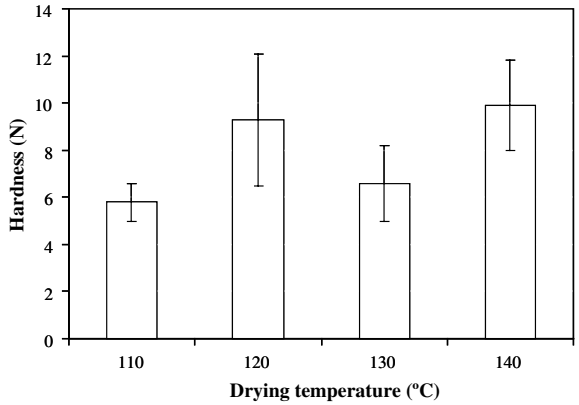

Fig. 8. Hardness of dried banana slices at different temperatures.

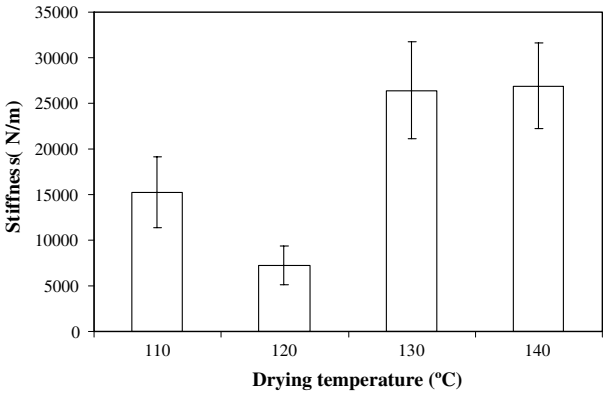

Fig. 9. Stiffness of dried banana slices at different temperatures.

The stiffness values were in the range of 2640–26,900 N/m when drying was performed at 130 and 140 °C and of 7200–15,000 N/m when drying was performed at 110 and 120 °C. According to theses values, it implied that banana slices were crispier when drying was performed at temperatures higher than 120 °C.

4. Conclusions

The drying rates of banana slices at high drying temperatures can be divided into three regimes, warming-up period and two falling rate periods. The effective moisture diffusion coefficients of bananas were found to vary with the temperature and moisture of the samples. The formation of large pore assembly, as revealed by scanning electron microscopy, was noted at a higher drying temperature of 120 °C. The formed large pores led further to lower shrinkage, due to the formation of rigid outer structure. In addition, the values of the stiffness were significantly higher when drying was performed at higher temperatures of 120 °C whereas the hardness of dried banana slices was insignificantly affected by the drying temperature. Although some physical properties were superior, higher-temperature drying induced greater changes of banana colors as indicated by the lower *L*- and higher *a*-values. The colors of banana slices became especially brown when drying was in the second falling rate period.

Acknowledgements

The authors express their appreciation to the Commission on Higher Education and the Thailand Research Fund (TRF) for financial support. Thanks are also due to the Institute of Food Research and Product Development (IFRPD) of Kasetsart University, Thailand, for testing textural properties of the samples.

References

Anon (1972). Banana ripening guide. Rep. No. circular 8. Collingwood, Australia: Division of Food Research, Commonwealth Scientific and Industrial Research Organisation.

Barreiro, J. A., Milano, M., & Sandoval, A. J. (1997). Kinetics of color change of double concentrated tomato paste during thermal treatment. *Journal of Food Engineering, 33*, 359–371.

Crank, J. (1975). *The mathematics of diffusion*. New York: Oxford University Press.

Del Valle, J. M., Cuadros, T. R. M., & Aguilera, J. M. (1998). Glass transitions and shrinkage during drying and storage of osmosed apple pieces. *Food Research International, 31*, 191–204.

Dinand, E., Chanzy, H., & Vignon, M. R. (1999). Suspensions of cellulose microfibrils from sugar beet pulp. *Food Hydrocolloids, 13*, 275–283.

Feng, H., & Tang, J. (1998). Microwave finish drying of diced apples in a spouted bed. *Journal of Food Science, 63*, 679–683.

Guillard, V., Broyart, B., Guilbert, S., Bonazzi, C., & Gontard, N. (2004). Moisture diffusivity and transfer modeling in a dry biscuit. *Journal of Food Engineering, 64*, 81–87.

Hofsetz, K., & Lopes, C. C. (2005). Crispy banana obtained by the combination of a high temperature and short time drying stage and a drying process. *Brazilian Journal of Chemical Engineering, 22*, 285–292.

Ibarz, A., Pagán, S., & Garza, S. (1999). Kinetic models for colour changes in pear puree during heating at relatively high temperatures. *Journal of Food Engineering, 39*, 415–422.

Jannot, Y., Talla, A., Nganhou, J., & Puiggali, J. R. (2004). Modeling of banana convective drying by the drying characteristic curve (DCC) method. *Drying Technology, 22*, 1949–1968.

Karathanos, V. T., Villalobos, G., & Saravacos, G. D. (1990). Comparison of two methods of estimation of the effective moisture diffusivity from drying data. *Journal of Food Science, 55*, 218–231.

Krokida, M. K., Tsami, E., & Urbricain, M. J. (1998). Kinetics on colour changes during drying of some fruits and vegetables. *Drying Technology, 16*, 667–685.

Li, Y. B., Seyed-Yagoobi, J., Moreira, R. G., & Yamsaengsung, R. (1999). Superheated steam impingement drying of tortilla chips. *Drying Technology, 17*, 191–213.

Lopez, A., Pique, M. T., Boatella, J., Romero, A., Ferran, A., & Garcia, J. (1997). Influence of drying conditions on the hazelnut quality: III. Browning. *Drying Technology, 15*, 989–1002.

Lozano, J. E., Rotstein, E., & Urbricain, M. J. (1983). Shrinkage, porosity and bulk density of food stuffs at changing moisture contents. *Journal of Food Science, 48*, 1497–1502.

Markowski, M., Cenkowski, S., Hatcher, D. W., Dexter, J. E., & Edwards, N. M. (2003). The effect of superheated-steam dehydration kinetics on textural properties of Asian noodles. *Transactions of the ASAE, 46*, 389–395.

Márquez, G., & AnWón, M. C. (1986). Influence of reducing sugars and amino acids in the color development of fried potatoes. *Journal of Food Science, 51*, 157–160.

Maskan, M. (2000). Microwave/air and microwave finish drying of banana. *Journal of Food Engineering, 44*, 71–78.

Maskan, M. (2001). Kinetics of color change of kiwifruits during hot air and microwave drying. *Journal of Food Engineering, 48*, 169–175.

Mayor, L., & Sereno, A. M. (2004). Modelling shrinkage during convective drying of food materials: a review. *Journal of Food Engineering, 61*, 373–386.

Mowlah, G., Takano, K., Kamoi, I., & Obara, T. (1983). Water transport mechanism and some aspects of quality changes during air drying of bananas. *Lebensmittel- Wissenschaft und-Technologie, 16*, 103–107.

Panyawong, S., & Devahastin, S. (2007). Determination of deformation of a food product undergoing different drying methods and conditions via evolution of a shape factor. *Journal of Food Engineering, 78*, 151–161.

Ramesh, M. N. (2003). Moisture transfer properties of cooked rice. *Lebensmittel-Wissenschaft und-Technologie, 36*, 245–255.

Sankat, C. K., Castaigne, F., & Maharaj, R. (1996). The air drying behaviour of fresh and osmotically dehydrated banana slices. *International Journal of Food Science and Technology, 31*, 123–135.

Sano, Y., & Yamamoto, S. (1990). Calculation of concentration-dependent mutual diffusion coefficient in desorption of film. *Journal of Chemical Engineering of Japan, 23*, 331–338.

Silva, D. C., & Luh, B. S. (1978). Scanning electron microscopy studies on starch granules of red kidney beans and bean spouts. *Journal of Food Science, 43*, 1405–1408.

Tong, C. H., & Lund, D. B. (1990). Effective moisture diffusivity in porous materials as a function of temperature and moisture content. *Biotechnology Progress, 6*, 67–75.

Tsami, E., & Katsioti, M. (2000). Drying kinetics for some fruits: Predicting of porosity and color during dehydration. *Drying Technology, 18*, 1559–1581.

Wang, N., & Brennan, J. G. (1995). Changes in structure, density and porosity of potato during dehydration. *Journal of Food Engineering, 24*, 61–76.

Yoshida, S., Imakoma, H., & Okazaki, M. (1991). Determination of diffusivity using the characteristics function for the regular regime. *Journal of Chemical Engineering of Japan, 24*, 720–726.

Available online at www.sciencedirect.com
ScienceDirect
Journal of Food Engineering 86 (2008) 573–583
JOURNAL OF FOOD ENGINEERING
www.elsevier.com/locate/jfoodeng

Drying characteristics and quality of banana foam mat

Ratiya Thuwapanichayanan [a,*], Somkiat Prachayawarakorn [b], Somchart Soponronnarit [a]

[a] School of Energy, Environment and Materials, King Mongkut's University of Technology Thonburi, 126 Pracha u-tid Road, Bangkok 10140, Thailand
[b] Department of Chemical Engineering, King Mongkut's University of Technology Thonburi, 126 Pracha u-tid Road, Bangkok 10140, Thailand

Received 12 July 2007; received in revised form 13 November 2007; accepted 14 November 2007
Available online 22 November 2007

Abstract

The combination of foaming and drying is an alternative method to produce crisp banana chips. The influences of whipping time and egg albumen concentration on the foam density were studied. The influences of foam density, drying temperature and egg albumen concentration on the drying characteristics and qualities of the final products in terms of shrinkage, texture and microstructure were subsequently evaluated. Banana puree with egg albumen, which was used as the foaming agent, was foamed to the densities of 0.3, 0.5 and 0.7 g/cm^3. Banana foam mats with 5 mm thickness were then dried to the moisture content of 0.03 kg/kg db at 60, 70 and 80 °C and superficial air velocity of 0.5 m/s. The experimental results showed that the extensive porous structure of foams with lower densities resulted in higher drying rates, moisture diffusivities and shrinkage. Dried banana foams with lower foam densities also had lower hardness and crispness values. The drying temperature and the egg albumen concentration did not influence the textural properties of the final products, however. To produce banana chips, the initial foam density of 0.5 g/cm^3 and drying temperature of 80 °C were recommended.
© 2007 Elsevier Ltd. All rights reserved.

Keywords: Crispness; Egg albumen; Microstructure; Moisture diffusivity; Shrinkage

1. Introduction

Bananas generally deteriorate rapidly after harvesting. The production of banana chips is an alternative way to preserve the quality and also to add value to bananas. Banana chips can be produced by various conventional methods, e.g., frying and hot air drying. However, there are some limitations of each method. Reduction of nutritional values is observed in dried products (Matz, 1976). The longer drying time is also required for low-temperature air drying (Sankat et al., 1996; Demirel and Turhan, 2003; Nguyen and Price, 2007). Also, air drying may yield the non-crisp product since its moisture content cannot be reduced to the desired value, approximately 0.04 kg/kg db, by low-temperature drying. Although high-temperature drying can produce crisp products, browning of the products, which is accelerated by high-temperature may occur (Tsami and Katsioti, 2000).

Vickers and Bourne (1976) demonstrated that dry crisp foods probably consist of cells or cavities, which are usually filled with air and a structural phase or cell walls that are formed by a brittle matrix. The combination of foaming and hot air drying is thus a feasible option to produce crisp banana chips because banana foams are very porous. In addition, the products can be dried rapidly to 0.04 kg/kg db, even at low-temperature, due to the less dense structure of the foams (Garcia et al., 1988; Sankat and Castaigne, 2004).

Foaming is a process by which liquid or semi solid foods are whipped to form foams. Many foods, e.g., egg white, beef extract and milk, naturally contain soluble proteins, which can be converted into stable foams when being whipped (Hart et al., 1963). Soluble proteins, known as foaming agents, contribute to the formation and stability of the foam structure. Proteins move through the aqueous phase and are spontaneously adsorbed at the air–aqueous interface where the viscoelastic films are subsequently formed. The outcome of proteins adsorption is a reduction in surface tension, which improves the foam formation

* Corresponding author. Tel.: +66 2 470 8695; fax: +66 2 470 8663.
E-mail address: t_ratiya@yahoo.com (R. Thuwapanichayanan).

0260-8774/$ - see front matter © 2007 Elsevier Ltd. All rights reserved.
doi:10.1016/j.jfoodeng.2007.11.008

(Prins, 1988). Moreover, the viscoelastic films are generally resistant to rupture and coalescence of gas bubbles dispersed in the liquid phase (Cherry and Mcwatters, 1981; Karim and Wai, 1999a).

Banana purees need to be incorporated with a foaming agent in order to be whipped to produce foams. Several foaming agents such as modified soybean protein (Gunther's D-100) (Bates, 1964), soy protein isolate (ICN Biomedicals) (Sankat and Castaigne, 2004) and dried egg albumen (Garcia et al., 1988) can be used to produce foamed bananas. Foams must also retain the open structure during drying. If foam breaks or drains excessively, increase in the drying time and poor product qualities, e.g., extreme shrinkage, may occur (Hart et al., 1963).

As mentioned earlier, the foam structure plays a major role in moisture movement during drying and also on subsequent product quality. Most prior works have emphasized on the drying characteristics of foamed foods (Cooke et al., 1976; Garcia et al., 1988; Karim and Wai, 1999b; Sankat and Castaigne, 2004) and Fick's law of diffusion, assuming constant moisture diffusivity, was used to describe the moisture content evolution during drying. In spite of its importance, the information on the quality of dried foamed products has received much less attention, however.

The objectives of this work were therefore to study the effects of whipping time and egg albumen concentration on the foam density. Subsequently, the effects of foam density, drying temperature and egg albumen concentration on the drying characteristics and the qualities of the final products in terms of shrinkage, texture and microstructure were evaluated. The effective moisture diffusivity of the foams was also determined by the method of slope.

2. Materials and methods

2.1. Preparation of banana puree and foam

Gros Michel bananas (*Musa Sapientum* L.) at a mature stage of 5, which contained total soluble solids of approximately 23–25° Brix were used. Bananas were cut into slices with a slicing machine. To prevent discoloration during foaming, the sliced bananas were pretreated by immersing them in 1% (w/w) sodium metabisulphite solution for 2 min and then rinsed with distilled water for 30 s (Krokida et al., 2000). The pretreated banana slices were chopped into small pieces and then blended in a blender (Waring, model no. 8011 BU, Torrington, CT) for 1 min. About 800 g of the banana puree was then poured into a mixing bowl and fresh egg albumen, which was used as the foaming agent, was added to the banana puree at 2%, 5% and 10% (on a wet puree basis). The banana puree with egg albumen was whipped with a Kitchen Aid Mixer (model no. 5K5SS, Strombeek-Bever, Belgium) at its maximum speed to the foam densities of 0.3, 0.5 and 0.7 g/cm^3.

Foam density was determined by measuring the mass of a fixed volume of the foam. The determination was performed carefully to avoid destroying the foam structure and to ensure that there were no voids while filling the foam into the measuring beaker. The experiments were done in duplicate.

The moisture content of the foamed bananas was determined by the vacuum oven method 934.06 (AOAC, 1995).

2.2. Drying procedure

Based on the observation of the foam density, egg albumen at concentrations of 5% and 10% could produce the lowest foam density of 0.3 g/cm^3. Both 5% and 10% of egg albumen were thus chosen to study the drying behavior of the foams.

Banana foam mats with a thickness of 5 mm were placed on a mesh tray, which was covered with aluminum foil, and then put into the drying chamber. The samples at three foam densities of 0.3, 0.5 and 0.7 g/cm^3 were then dried to about 0.03 kg/kg db using the drying air temperatures of 60, 70 and 80 °C and a superficial air velocity of 0.5 m/s. Moisture loss from the samples was determined by weighing the sample tray outside the drying chamber using an electronic balance (±0.01 g).

2.3. Determination of shrinkage

Four banana foam mats taken at different drying times were measured for their volumes. The volume was determined by the volumetric displacement method using glass beads with a diameter in the range of 0.106–0.212 mm as a replacement medium (Hwang and Hayakawa, 1980). In each measurement, one sample piece was used and the mean value of four samples was reported.

The volume ratio was used to describe shrinkage, which is defined as

$$\text{Volumetric Shrinkage} = V/V_0 \tag{1}$$

where V is the volume of the sample after drying (cm^3) and V_0 is the initial volume of the sample before drying (cm^3).

2.4. Texture analysis

The texture of dried banana foam mats was evaluated by a compressive test using a texture analyzer model TA.XT.plus (Stable Micro Systems, Surrey, UK). The sample was placed on the hollow planar base. The test applied a direct force to the sample using a 5 mm spherical probe at a constant crosshead speed of 2 mm/s. The hardness was defined as the maximum force in the force–deformation curve while the crispness was characterized by the number of peaks and the slope of the first peak. Eight samples were tested and the average values of hardness and crispness were reported.

2.5. Microstructural analysis

A scanning electron microscope (JEOL JSM-5600LV, Tokyo, Japan) was used to study the microstructure of dried

banana foam mats. The dried banana foam mats were placed on two-side adhesive tape attached to metal stubs and were coated with gold. SEM micrographs were taken at an accelerating voltage of 10 kV and a magnification of 35×.

2.6. Image analysis

To quantify the porous foam characteristics such as pore diameter and pore area, image analysis software (ImagePro + 5.0, MediaCybernetic, MD, USA) was used. Each pixel of SEM micrograph was assigned a value of gray intensity (0–255). Threshold-based segmentation technique was employed to distinguish the pore from the solid phase with an appropriate gray level threshold. A binary image was then generated. The pixels with gray levels lower than the selected threshold were assigned as pore, which appeared as black color in a binary image while the pixels with gray levels above the selected threshold were set as solid phase, which appeared as white color in a binary image. With an assumption of spherical shape, a pore diameter was estimated from the known pore area. The pore area was determined by counting the number of pixels filled in the specified space.

2.7. Statistical analysis

The data were analyzed using the analysis of variance (ANOVA). Duncan's test was used to establish the multiple comparisons of mean values. Mean values were considered at 95% significance level ($p < 0.05$).

3. Determination of moisture diffusivity

For the effective moisture diffusivity determination, banana foam mats were assumed to be infinite slabs. In addition, moisture movement during drying occurred only in the direction of material thickness. The external resistance to moisture transfer was negligible and the moisture distribution inside banana foams before drying was uniform.

When the plot of logarithm of moisture ratio (ln MR) versus drying time is linear, the moisture diffusivity assumes an independent function of moisture content. In this case, the change of moisture content can be described by the following equation (Crank, 1975):

$$\mathrm{MR} = \frac{M - M_{\mathrm{eq}}}{M_0 - M_{\mathrm{eq}}} = \frac{8}{\pi^2}\sum_{n=0}^{\infty}\frac{1}{(2n+1)^2}\exp\left[-\frac{(2n+1)^2\pi^2 Dt}{4L^2}\right] \quad (2)$$

where D is the effective moisture diffusivity (m^2/s), MR is the moisture ratio, M, M_{eq} and M_0 are the average, equilibrium and initial moisture contents (kg/kg db), respectively. Since the top surface of banana foam mats were only exposed to hot air, the length, L, in Eq. (2) was the thickness of the slabs.

In case of non-linear experimental drying curves, however, the effective moisture diffusivity is dependent on moisture content, which is usually the case for highly porous materials (Hamdami et al., 2004; Sakin et al., 2007). In such case, the effective moisture diffusivity at various moisture contents can be estimated using the method of slope (Karathanos et al., 1990). The calculation was based on the ratio of the slopes of the experimental drying curves to the slopes of the theoretical curves at the same moisture contents. The slopes of the experimental drying curves were calculated using experimental data points while the slopes of the theoretical curves were calculated by differentiating Eq. (2) with respect to Fo ($\mathrm{dMR}/\mathrm{d}Fo$). The effective moisture diffusivity at a given moisture was then estimated by the following equation:

$$D_{\mathrm{eff}} = [(\mathrm{dMR}/\mathrm{d}t)_{\mathrm{exp}}/(\mathrm{dMR}/\mathrm{d}Fo)_{\mathrm{th}}]L^2 \quad (3)$$

where Fo is the Fourier number, $Fo = D_{\mathrm{eff}}t/L^2$.

Since the thickness of banana foam mats changed during drying, L in Eq. (3) varied with time.

4. Results and discussion

4.1. Foam density

The effects of whipping time and concentration of egg albumen on the foam density are shown in Fig. 1. During the whipping process, air was brought into the liquid puree and entrapped in the liquid as bubbles. This led to a decrease of foam density as the whipping time increased as shown in Fig. 1; banana puree of minimum density was formed after 20 min of whipping. Beyond this time the foam density increased rapidly. The pattern of the banana foam density curves during whipping is similar to that of other foods, which are high in viscosity such as tomato paste foam. Labelle (1966) reported that tomato paste with 1% myverol used as foaming agent was foamed to the minimum density after 4 min of whipping; this was followed by an increase in the foam density. The increase in foam density was attributed to more liquid film thinning,

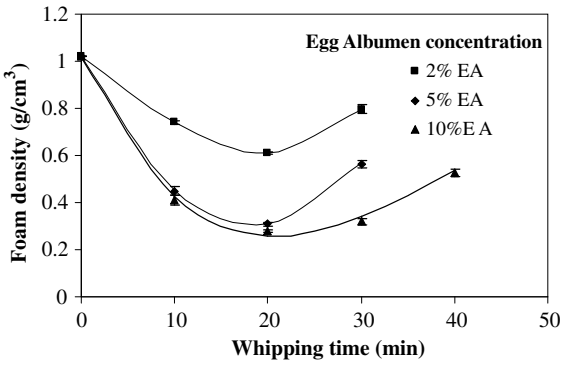

Fig. 1. Foam density as a function of fresh egg albumen (EA) concentration and whipping time.

more mechanical deformation and more bubble wall rupture during extended whipping (Lau and Dickinson, 2005).

As the concentration of egg albumen increased, the foam density decreased (Fig. 1). The foam density decreased to approximately 0.6, 0.3 and 0.27 g/cm^3 after 20 min of whipping when using egg albumen concentrations of 2%, 5% and 10% (w/w), respectively. The high banana foam densities at low egg albumen concentrations were due to the fact that the movement of the foaming agent from the aqueous phase towards the air–aqueous interface was limited (Karim and Wai, 1999a), insufficient for the reduction in surface tension, which enhances the foam formation.

However, excessive egg albumen concentration beyond a certain value did not further reduce the foam density. As shown in Fig. 1, an increase in the egg albumen concentration from 5% to 10% led to lower foam density only by 3% whilst an increase in the egg albumen concentration from 2% to 5% could lower the foam density by up to 30%. The only slightly lower foam density when the egg albumen concentration increased from 5% to 10% might be due to the saturation of egg albumen solubility in banana puree under the given set of experimental conditions. The egg albumen solubility depends on the type of foods. Rajkumar et al. (2005) indeed reported that the egg albumen solubility in mango foam was in the range of 10–15%.

4.2. Drying characteristics of banana foam mats

The influences of foam density, drying temperature and egg albumen concentration on the drying characteristics of banana foam mats were studied. Fig. 2a–c shows the drying curves of banana foam mats at different initial foam densities using 5% egg albumen concentration. When the foamed bananas were dried at 60 °C, the time required for reducing their moisture content to about 0.03 kg/kg db was 120 and 300 min for the initial foam densities of 0.3 and 0.5 g/cm^3, respectively. Beyond the initial foam density of 0.5 g/cm^3, the required drying time was much longer than 540 min. As the drying temperature increased to 80 °C, the drying time was shorter by approximately 50%. These results show the importance of foam density and drying temperature on the moisture movement in which the diffusion of water through the low density foam was much easier and became faster when the higher drying temperatures were used.

The drying rate data presented in Fig. 3a–c show the presence of a heat up period at the early stage of drying (H); this was then followed by the falling rate period. In the heat up period, the drying rates increased as the moisture content of banana foam mats decreased from the initial moisture content to approximately 2.6 kg/kg db. Thereafter, the drying rates decreased with decreasing moisture content, signalling the beginning of the falling rate period. The falling rate period could be divided into two periods according to the change in the drying rate

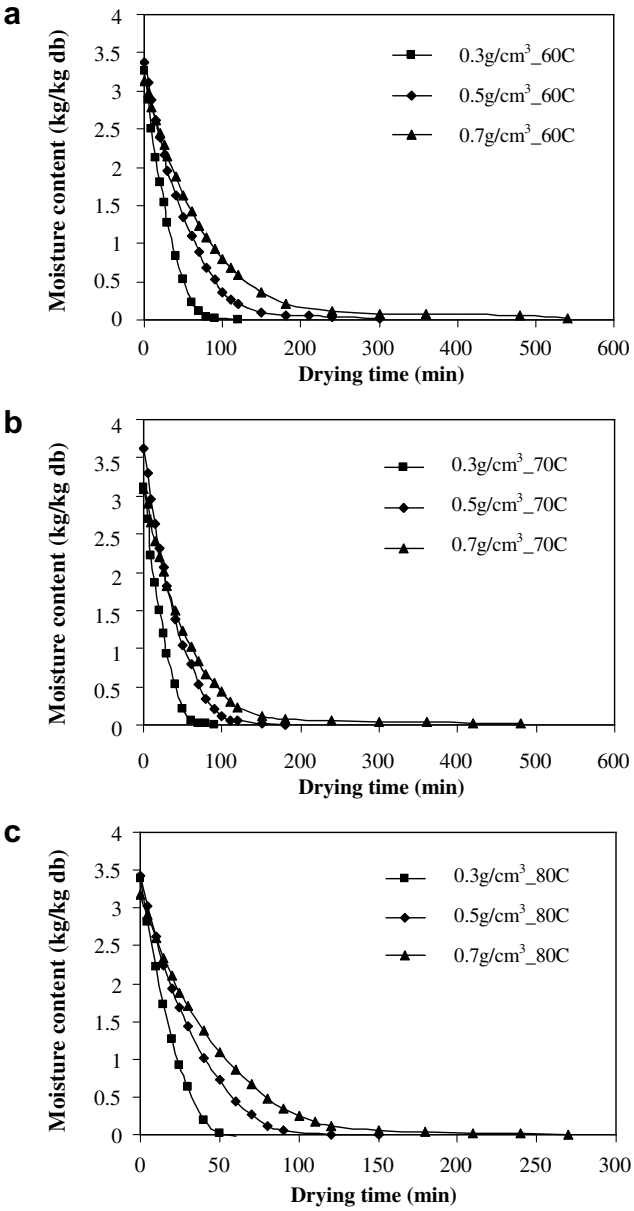

Fig. 2. Drying curves of banana foam mats at different initial foam densities and drying temperatures (5 mm foam thickness, at a superficial air velocity of 0.5 m/s and egg albumen concentration of 5%).

curves. First falling rate period (I), occurring between the moisture content of 0.35 and 2.6 kg/kg db, corresponded to the loss of free water. This water was freely available around the solid matrices that could easily transport by capillary flow and vapor diffusion. However, the removal of the water from the interior of banana foam mats to the exposed surface was not fast enough to keep the surface moist. Thus, the drying rates in this period decreased gradually with decreasing moisture content. At moisture contents below 0.35 kg/kg db, a decrease in drying rate was sharper, indicating that the drying was in the second falling rate period (II). Lim et al. (1995) reported that the moisture content corresponding to the bound water ranges from

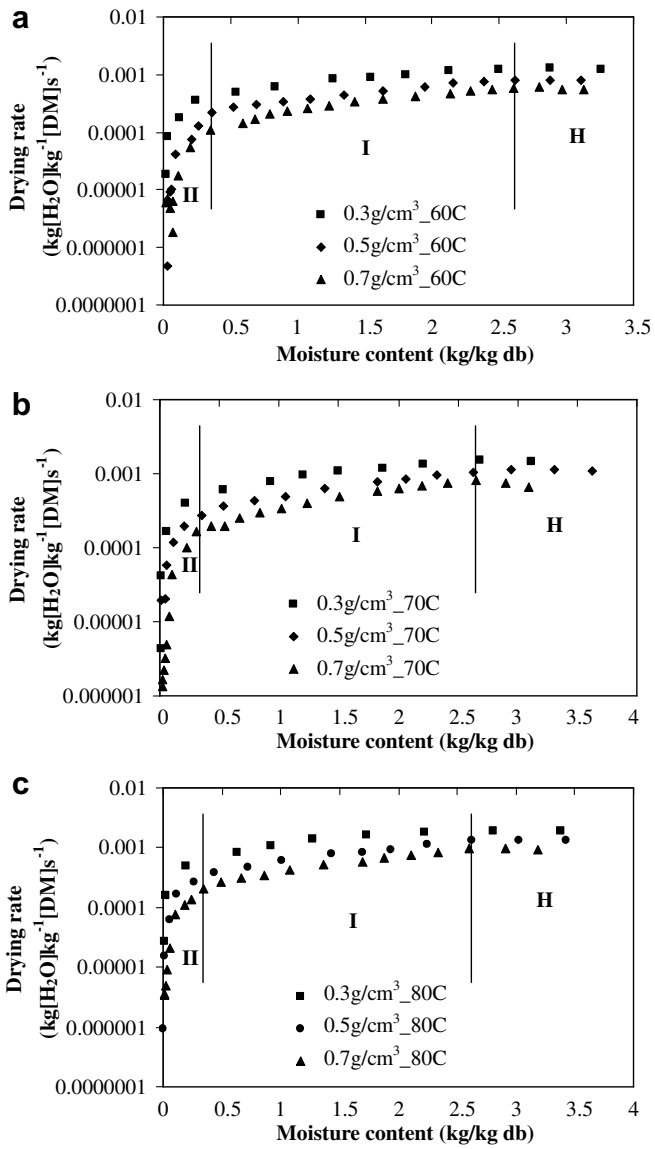

Fig. 3. Drying rate curves of banana foam mats at different initial foam densities and drying temperatures (5 mm foam thickness, at a superficial air velocity of 0.5 m/s and egg albumen concentration of 5%).

0.11 kg/kg db to 0.21 kg/kg db, depending on the type of fruit. Thus, the very low drying rate in the second falling rate period is probably because small free water is available and the diffusion of bound water is the main mechanism controlling the water transport.

The structure of banana foams also played an important role on the internal mass transfer rates. For higher foam density, e.g., 0.7 g/cm^3, with small air voids, the quantity of water, which travelled through the void space was small. As the void space increased, leading to lower foam density, larger amount of water could travel. This led to higher values of the moisture diffusivity, resulting in high drying rates at lower foam densities as shown in Fig. 3a–c. In addition to the material structure, drying temperature also affected the drying rates. The drying rates of banana foam mats were higher when drying was performed at higher drying temperatures as can be seen in Fig. 3a–c.

Fig. 4 shows the drying curves of banana foam mats at 5% and 10% egg albumen concentrations. It can be seen that the egg albumen concentration had no significant effect on the drying characteristics whether drying was performed at lower or higher temperatures.

4.3. Effective moisture diffusivity

Fig. 5 shows the plot of logarithm of moisture ratio (ln MR) versus drying time of banana foam mats. It is evident that their relationship were non-linear. The non-linearity of the curves indicated the variation in effective diffusivity with moisture content.

The effective moisture diffusivity of banana foam mats was calculated from Eq. (3). The variation in effective diffusivity with moisture content is shown in Fig. 6a and b. At the initial stage of drying, the effective diffusivity increased with decreasing moisture content due to the rapid rise of product temperature. As drying progressed, the effective diffusivity decreased with decreasing moisture content. In addition to the moisture content, the effective moisture diffusivity was higher when the drying temperature increased and the initial foam density decreased.

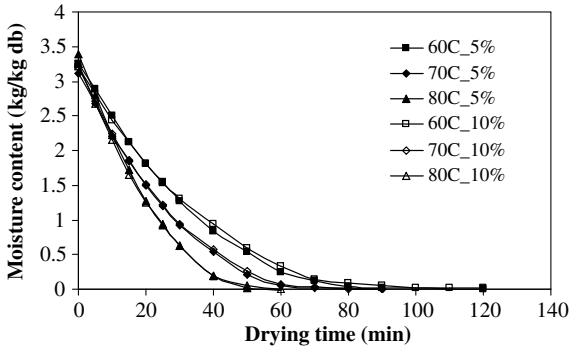

Fig. 4. Drying curves of banana foam mats at different egg albumen concentrations and drying temperatures (5 mm foam thickness, initial foam density of 0.3 g/cm^3 and a superficial air velocity of 0.5 m/s).

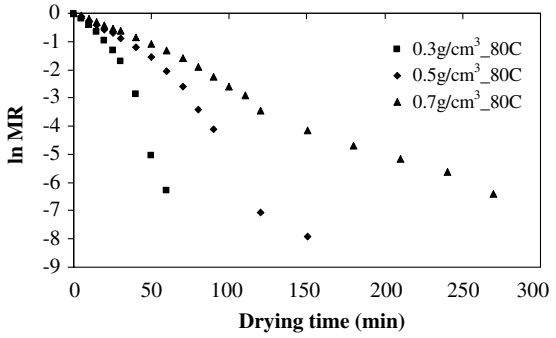

Fig. 5. Plot of logarithm of moisture ratio versus drying time of banana foam mats at different drying conditions (5 mm foam thickness, a superficial air velocity of 0.5 m/s and egg albumen concentration of 5%).

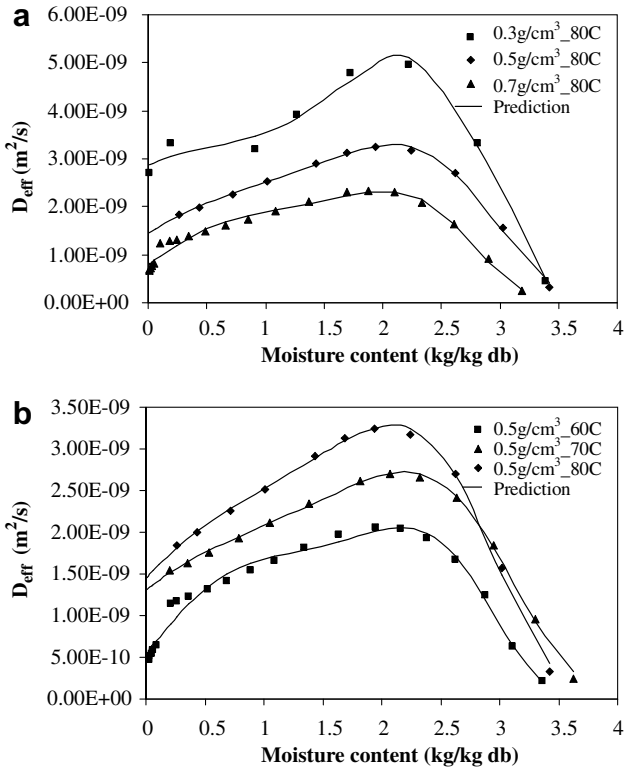

Fig. 6. Moisture diffusivity of banana foam mats at different drying conditions (5 mm foam thickness, a superficial air velocity of 0.5 m/s and egg albumen concentration of 5%).

The relationship between effective moisture diffusivity and moisture content of banana foams of various initial foam densities and drying temperatures is expressed by the following empirical equation:

$$D_{\text{eff}}(M) = a \exp\left(\sum_{i=1}^{4} \alpha_i M^i\right) \tag{4}$$

where a and α_i are the empirical parameters, which were obtained through non-linear regression analysis of the experimental data; the results together with R^2 values are presented in Table 1. The proposed equation could adequately describe the relationship between the effective moisture diffusivity and moisture content of banana foams.

Table 2
Average effective moisture diffusivity and activation energy at various drying conditions

Drying condition		$D_{\text{eff,avg}}$ (m^2/s)	Activation energy, E_a (kJ/mol)	R^2
Foam density (g/cm^3)	Temperature (°C)			
0.3	60	2.34×10^{-9}	21.08	0.997
	70	2.86×10^{-9}		
	80	3.60×10^{-9}		
0.5	60	1.49×10^{-9}	22.90	0.989
	70	1.98×10^{-9}		
	80	2.38×10^{-9}		
0.7	60	1.02×10^{-9}	25.19	0.973
	70	1.43×10^{-9}		
	80	1.70×10^{-9}		

4.4. Activation energy of banana foams

The activation energy of banana foams could be obtained through an Arrhenius type relationship, for which the average effective moisture diffusivity, $D_{\text{eff,avg}}$, relates to the drying air temperature:

$$D_{\text{eff,avg}} = D_0 \exp\left(\frac{-E_a}{RT_{\text{abs}}}\right) \tag{5}$$

where D_0 is the constant value (m^2/s), E_a is the activation energy (kJ/kmol), R is the universal gas constant (8.314 kJ/kmol K) and T_{abs} is the absolute drying air temperature (K).

In order to estimate the activation energy, it is necessary to calculate the average effective moisture diffusivity from D_{eff} versus M curves. This can simply be done through the use of the following equation:

$$D_{\text{eff,avg}} = \frac{\int_{M_{\text{initial}}}^{M_{\text{final}}} D_{\text{eff}}(M)\mathrm{d}M}{\int_{M_{\text{initial}}}^{M_{\text{final}}} \mathrm{d}M} \tag{6}$$

The values of $D_{\text{eff,avg}}$ of all drying conditions are presented in Table 2. The average effective moisture diffusivity increased when the drying temperature increased and the initial foam density decreased, as expected.

Table 1
Calculated values of a and α_i (Eq. (4)) for various foam densities and drying temperatures

Drying condition		Empirical parameter					
Foam density (g/cm^3)	Temperature (°C)	$a \times 10^{-10}$	α_1	α_2	α_3	α_4	R^2
0.3	60	20.4978	0.3823	−0.750	0.6042	−0.138	0.980
	70	25.4514	0.5247	−1.013	0.7768	−0.177	0.964
	80	28.5214	0.4324	−0.602	0.5060	−0.121	0.983
0.5	60	5.5042	2.8784	−2.8579	1.3158	−0.2218	0.974
	70	12.9837	0.8666	−0.6938	0.3734	−0.0763	0.998
	80	14.5071	1.0528	−0.8794	0.476	−0.099	0.996
0.7	60	3.3549	3.1578	−3.2075	1.5468	−0.2762	0.953
	70	4.4478	3.7392	−4.0588	1.9792	−0.3497	0.945
	80	7.879	2.2188	−2.2754	1.1498	−0.2157	0.973

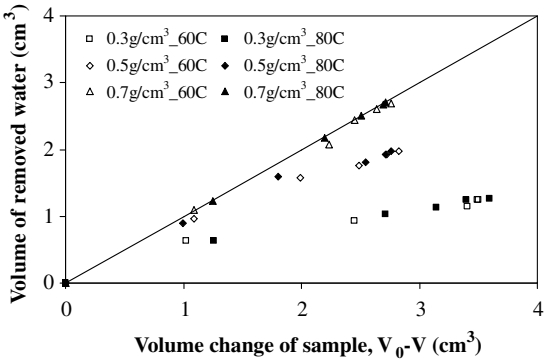

Fig. 7. Volume of removed water versus volume change of sample (V_0 is the initial volume of sample and V is the volume of sample at different drying times).

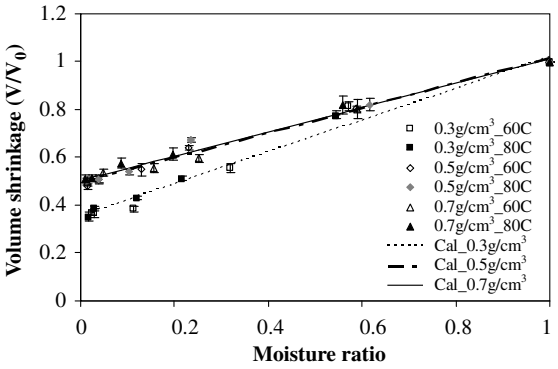

Fig. 8. Volume shrinkage of banana foam mats at different initial foam densities and drying temperatures (5 mm initial foam thickness and egg albumen concentration of 5%).

The values of activation energy for banana foam mats are presented in Table 2. E_a was 21.08, 22.90 and 25.19 kJ/mol for foam densities of 0.3, 0.5 and 0.7 g/cm^3, respectively. E_a decreased with decreasing foam density; this indicated that at lower foam densities, water molecules could move easier than it could at higher foam densities.

The activation energy of the moisture diffusivity for hot air drying of banana slices was 34.7 ± 0.073 and 39.8 ± 4.6 kJ/mol when using the slab thickness of 1 cm and 2 cm, respectively. This indicates the unimportant effect of thickness on the activation energy (Nguyen and Price, 2007). According to this information, drying of banana slices requires higher energy for driving water out than did the banana foam mats.

4.5. Shrinkage of banana foams

As shown in Fig. 7, shrinkage or volume change of the samples at an initial foam density of 0.7 g/cm^3 fully compensated the volume of removed water, as indicated by the experimental data close which lie to the diagonal line. In the case of low density foams, e.g., at initial foam densities of 0.3 and 0.5 g/cm^3, shrinkage of such systems was accompanied by bubble collapse since the foam was non-rigid during drying. In such cases, shrinkage was more significant than the volume of removed water, as indicated by their values deviating from the diagonal line. The largest deviation could be observed when using an initial foam density of 0.3 g/cm^3. These results indicate that shrinkage of lower density foam was due to the collapse of gas bubbles, besides the stress formation within the foams.

Fig. 8 shows the volume shrinkage of banana foams of different initial foam densities; the effect of drying temperature was also shown here. The drying temperature insignificantly affected shrinkage of the samples of the same foam density. This is probably because the tested drying temperature (60–80 °C) might not be much different to cause any significant differences on the volume shrinkage. A decrease in the volume of banana foams was in a linear relation with the moisture content and its volume reduction could be described by the following equation:

$$V/V_0 = a + bM/M_0 \quad (7)$$

The values of parameters a and b were obtained by linear regression analysis of the experimental data. Both empirical parameters depended on the initial foam densities; the results are given in Table 3.

4.6. Texture of banana foams

The texture of banana foams was evaluated by a compressive test. The maximum force of rupture is defined as the hardness. The number of peaks was counted when that peak had a value higher than the threshold value, which was set at 30 g, and the slope of the first peak or steepness was used to describe the crispness of the samples. A crisp chip had a steep slope, representing more resistance to bending than a less crisp chip.

Banana foam mats, after drying to about 0.03 kg/kg db, except for samples with initial foam density of 0.7 g/cm^3 and dried at 60 °C, which its final moisture content was 0.05 kg/kg db, were taken to examine their textural properties. It was noted that the textural properties were strongly affected by the sample porous structure. The samples with initial foam density of 0.3 g/cm^3, characterized by a number of larger pores and more limited number of smaller pores, yielded the less dense structure and lower strength. Hence, hardness was smaller as compared with that of

Table 3
Calculated values of a and b (Eq. (7)) for various foam densities

$\rho_f = 0.3$ g/cm^3			$\rho_f = 0.5$ g/cm^3			$\rho_f = 0.7$ g/cm^3		
a	b	R^2	a	b	R^2	a	b	R^2
0.349	0.702	0.977	0.496	0.521	0.983	0.503	0.507	0.984

the samples with higher initial foam densities (see Fig. 9a). For example, the maximum forces of samples dried at 80 °C were 2.23 ± 0.28 Fig. 9a, 5.90 ± 0.72 Fig. 9b and 18.06 ± 3.51 Fig. 9c N when using initial foam densities of 0.3, 0.5 and 0.7 g/cm^3, respectively.

In terms of crispness, which is a desired textural characteristic of chips, the samples with lower initial foam densities had smaller numbers of peaks and lower slopes of the first peak as shown in Fig. 9b and c. The numbers of peaks of samples dried at 80 °C were 7 ± 2 Fig. 9a, 16 ± 3 Fig. 9b and 20 ± 7 Fig. 9c when using initial foam densities of 0.3, 0.5 and 0.7 g/cm^3, respectively, and the slopes of the first peak of the samples dried at 80 °C were 3.58 ± 2.06 Fig. 9a, 11.00 ± 1.89 Fig. 9b and 19.03 ± 6.47 Fig. 9c N/mm for samples with initial foam densities of 0.3, 0.5 and 0.7 g/cm^3, respectively. The small number of peaks and low initial slope obtained for samples at low initial foam density of 0.3 g/cm^3 indicated that this banana foam was less crisp as compared with the samples produced with higher initial foam densities.

Although the very porous structure was obtained for sample with the lowest initial foam density, the product was not crisp. These textural properties, in particular the steepness, were similar to those of freeze dried chips. Sham et al. (2001) found that freeze dried apple chips, with their very porous structure, were spongy and not crisp. As shown in Figs. 9 and 10, the drying temperature and egg albumen concentration did not influence the hardness and crispness. These results suggest that 5% egg albumen concentration is suitable for preparing banana foams and that drying should be conducted at the highest temperature in order to save the time and energy consumption.

As mentioned earlier, the low density of banana foams could lead to the soft texture but the high density, on the other hand, led to the hard texture. Too soft and too hard textures may not be suitable for crisp product. The commercial cracker (Hi Crack™) was examined for its textural properties and it was found that the values of the maximum force and number of peaks were 7.9 ± 1.23 and 10 ± 5 N, respectively. Both values corresponded to those

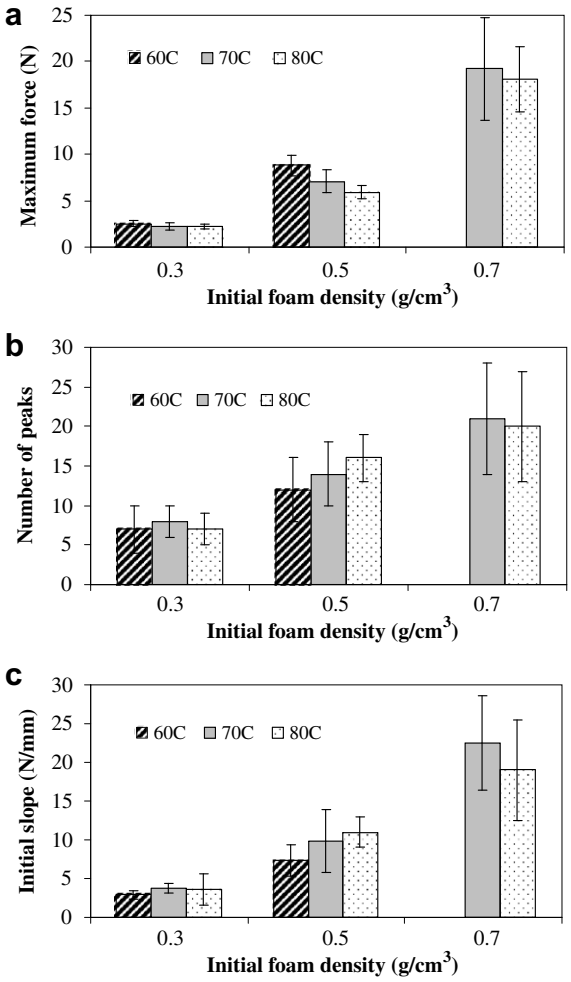

Fig. 9. Effect of initial foam density and drying temperature on (a) maximum force, (b) number of peaks and (c) initial slope of dried banana foam mat (egg albumen concentration of 5%).

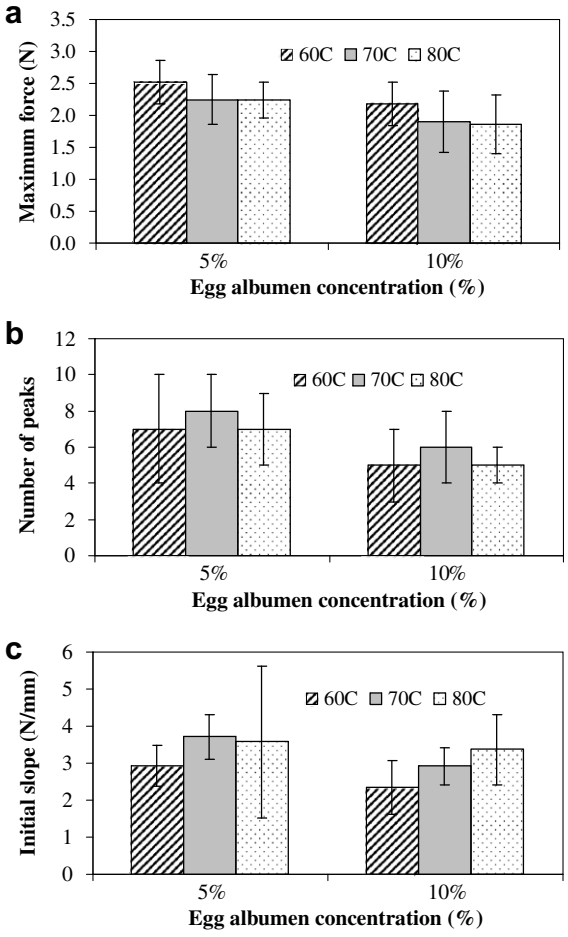

Fig. 10. Effect of egg albumen concentration on (a) maximum force, (b) number of peaks and (c) initial slope of dried banana foam mat (initial foam density of 0.3 g/cm^3).

of banana foam mats prepared with the initial foam density of 0.5 g/cm^3.

4.7. SEM micrographs and image analysis

SEM micrographs of banana foam mats containing 5% egg albumen and dried at different temperatures are shown in Fig. 11a–d for various initial foam densities. The binary images are illustrated in Fig. 11e–h. The reconstructed porous structure of the dried banana foam mats in binary images reproduced adequately their original images.

The pore shape of banana foams before drying was spherical (not shown here). When the samples were dried, the pore shape changed. As shown in Fig. 11, the pore shape of dried banana foam mats was elongate, probably due to the stress formation during drying, which led to some distortion.

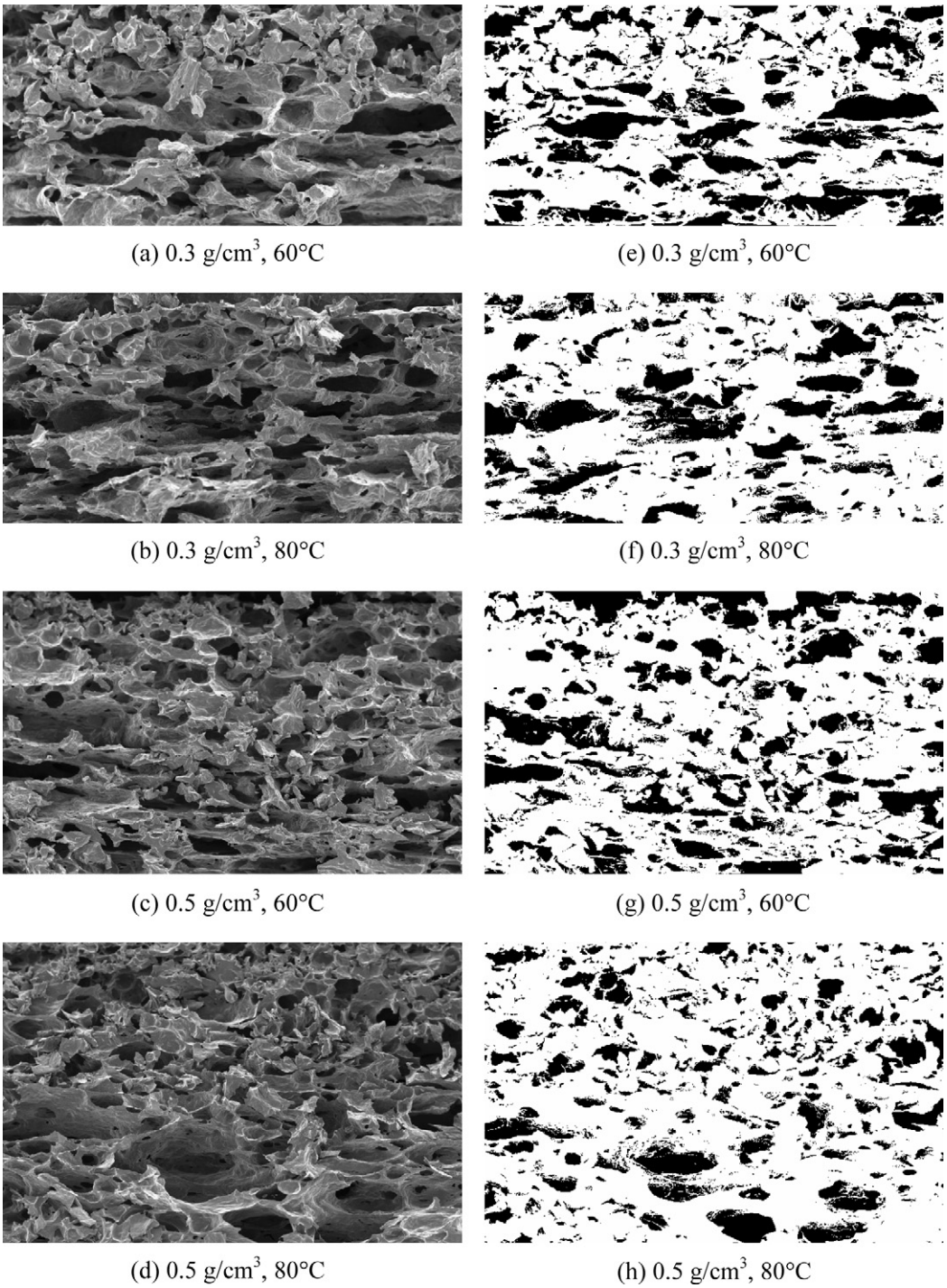

Fig. 11. (a–d) SEM micrographs of dried banana foam mats at different initial foam densities and drying temperatures and (e–h) binary image.

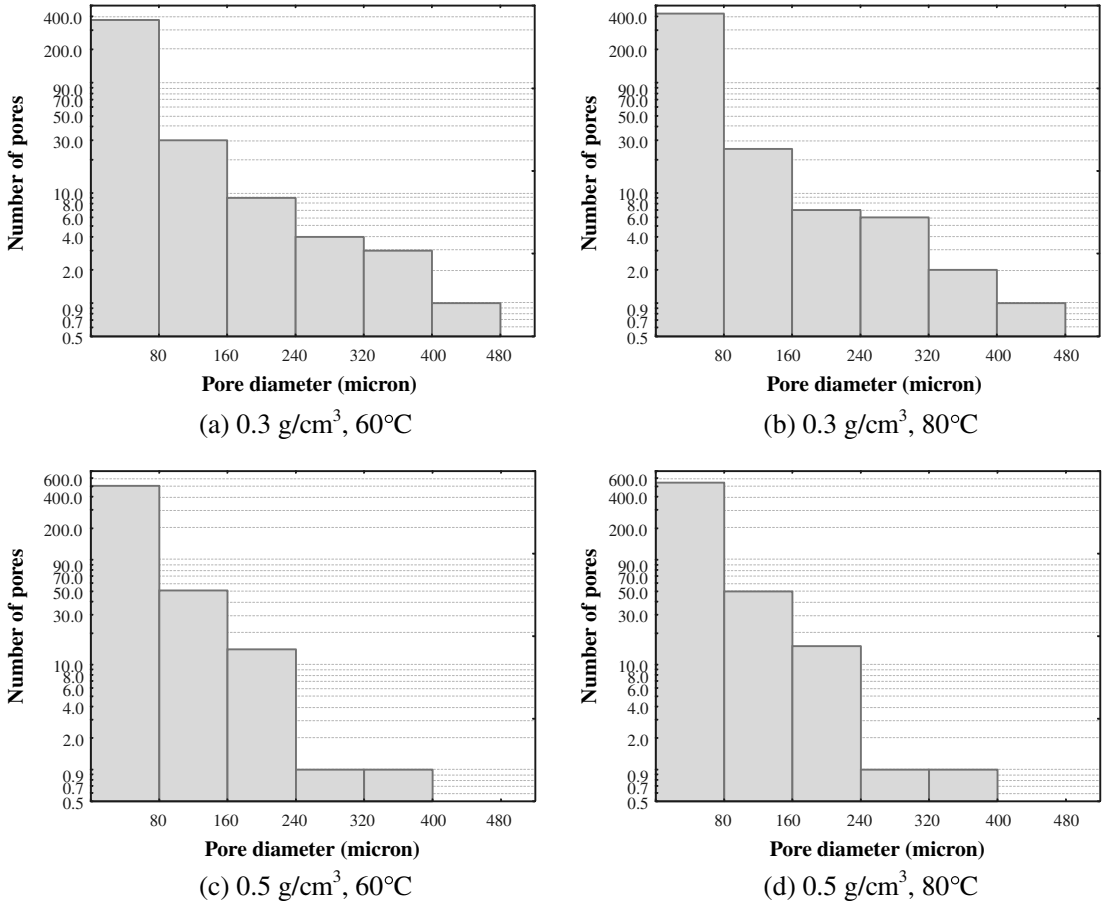

Fig. 12. Pore diameter distribution at different foam densities and drying temperatures.

The pore size distributions are shown in Fig. 12. The pore diameter was estimated from the known pore area by assuming a spherical shape. Considering the effect of initial foam density on the pore size of dried banana foam mats, it was observed that the samples with an initial foam density of 0.3 g/cm^3 had a larger number of large pores in the range of 240–480 μm than those at higher initial foam densities. This large pore assembly might probably be generated from the coalescence of adjacent bubbles. However, the number of small pores, ranging from 10 to 240 μm, was lesser as compared with the samples with an initial foam density of 0.5 g/cm^3. As shown in Fig. 12, the samples with an initial foam density of 0.5 g/cm^3 had no pores with diameters larger than 400 μm. Although the total number of pores was smaller for samples with an initial foam density of 0.3 g/cm^3, the void area fraction was relatively larger because of a greater number of large pore assemblies. The void area fraction of the samples dried at 60 °C was 22% and 18% for initial foam densities of 0.3 and 0.5 g/cm^3, respectively.

As shown in Fig. 12, the porous structure was insignificantly different amongst the samples dried at higher and lower temperatures. This corresponded to other qualities, i.e., shrinkage and textural properties, in which those qualities were not dependent on the drying temperature.

5. Conclusions

Addition of egg albumen at concentrations of 5% and 10% could produce low density banana foams of 0.3 g/cm^3 at an optimum whipping time of 20 min. Drying of banana foams mostly occurred in the falling rate period with higher drying rates at higher drying air temperatures and low foam densities. The initial foam density strongly affected the moisture diffusivity where the lower foam density, corresponding to larger void area and larger pore sizes of banana foams, provided higher values of effective diffusivity. In spite of efficient moisture transport, the very porous banana foams led to lower values of hardness and crispness. Shrinkage was also higher, except for the samples with initial foam densities beyond 0.5 g/cm^3. The drying temperature had no significant effect on the textural properties, morphology and shrinkage, however. To produce crispy banana chips, the initial foam density of 0.5 g/cm^3 and drying temperature of 80 °C was recommended.

Acknowledgement

The authors express their appreciation to the Thailand Research Fund (TRF) and the Commission on Higher Education for the financial support.

References

AOAC, 1995. Official Methods of Analysis, 16th ed. Association of Official Agricultural Chemists, Washington, DC.

Bates, R.P., 1964. Factors affecting foam production and stabilization of tropical fruit products. Food Technology 18, 93–96.

Cherry, J.P., Mcwatters, K.H., 1981. Whippability and aeration. In: Cherry, J.P. (Ed.), Protein Functionality in Foods. American Chemical Society, Washington, DC, pp. 149–176.

Cooke, R.D., Breag, G.R., Ferber, C.E.M., Best, P.R., Jones, J., 1976. Studies of mango processing I. The foam-mat drying of mango (*Alphonso cultivar*) puree. Journal of Food Technology 11, 463–473.

Crank, J., 1975. The Mathematics of Diffusion. Clarendon Press, Oxford.

Demirel, D., Turhan, M., 2003. Air-drying behavior of Draft Cavendish and Gros Michel banana slices. Journal of Food Engineering 59, 1–11.

Garcia, R., Leal, F., Rolz, C., 1988. Drying of bananas using microwave and air ovens. International Journal of Food Science and Technology 23, 73–80.

Hamdami, N., Monteau, J.Y., Bail, A.L., 2004. Transport properties of a high porosity model food at above and sub-freezing temperatures. Part 2: Evaluation of the effective moisture diffusivity from drying data. Journal of Food Engineering 62, 385–392.

Hart, M.R., Graham, R.P., Ginnette, L.F., Morgan, A.I., 1963. Foams for foam-mat drying. Food Technology 17, 1302–1304.

Hwang, M.P., Hayakawa, K.I., 1980. Bulk densities of cookies undergoing commercial baking processes. Journal of Food Science 45, 1400–1402.

Karathanos, V.T., Villalobos, G., Saravacos, G.D., 1990. Comparison of two methods of estimation of the effective moisture diffusivity from drying data. Journal of Food Science 55, 218–223.

Karim, A.A., Wai, C.C., 1999a. Characteristics of foam prepared from starfruit (*Averrhoa carambola* L.) puree by using methyl cellulose. Food Hydrocolloids 13, 203–210.

Karim, A.A., Wai, C.C., 1999b. Foam-mat drying of starfruit (*Averrhoa carambola* L.) puree. Stability and air drying characteristics. Food Chemistry 64, 337–343.

Krokida, M.K., Kiranoudis, C.T., Maroulis, Z.B., Marinos, D., 2000. Effect of pretreatment on color of dehydrated products. Drying Technology 18, 1239–1250.

Labelle, R.L., 1966. Characterization of foams for foam-mat drying. Food Technology 20, 89–94.

Lau, C.K., Dickinson, E., 2005. Instability and structural change in an aerated system containing egg albumen and invert sugar. Food Hydrocolloids 19, 111–121.

Lim, L.T., Tang, J., He, J., 1995. Moisture sorption characteristics of freeze dried blueberries. Journal of Food Science 60, 810–814.

Matz, S.A., 1976. Snack Food Technology. The AVI Publishing Company, Westport.

Nguyen, M.H., Price, W.E., 2007. Air-drying of banana: influence of experimental parameters, slab thickness, banana maturity and harvesting season. Journal of Food Engineering 79, 200–207.

Prins, A., 1988. Principles of foam stability. In: Dickinson, E., Stainsby, G. (Eds.), Advances in Food Emulsions and Foams. Elsevier Applied Science, New York, pp. 91–122.

Rajkumar, P., Kailappan, R., Raghavan, G.S.V., Vishwanathan, R., Ratti, C., 2005. Foam mat drying of mango pulp (Totapuri). In: Proceedings of the fourth Asia Pacific Drying Conference, vol. 1. Allied Publishers Pvt. Ltd., New Delhi, pp. 479–495.

Sakin, M., Ertekin, F.K., Ilicali, C., 2007. Modeling the moisture transfer during baking of white cake. Journal of Food Engineering 80, 822–831.

Sankat, C.K., Castaigne, F., Maharaj, R., 1996. The air drying behaviour of fresh and osmotically dehydrated banana slices. International Journal of Food Science and Technology 31, 123–135.

Sankat, C.K., Castaigne, F., 2004. Foaming and drying behaviour of ripe bananas. Lebensmittel-Wissenshaft und-Technologie 37, 517–525.

Sham, P.W.Y., Scaman, C.H., Durance, T.D., 2001. Texture of vacuum microwave dehydrated apple chips as affected by calcium pretreatment, vacuum level and apple variety. Journal of Food Science 66, 1341–1347.

Tsami, E., Katsioti, M., 2000. Drying kinetics for some fruits: predicting of porosity and color during dehydration. Drying Technology 18, 1559–1581.

Vickers, Z.M., Bourne, M.C., 1976. A psychoacoustical theory of crispness. Journal of Food Science 41, 1158–1164.

Available online at www.sciencedirect.com
ScienceDirect
International Journal of Heat and Mass Transfer 51 (2008) 344–352
International Journal of HEAT and MASS TRANSFER
www.elsevier.com/locate/ijhmt

Effects of pore size distribution and pore-architecture assembly on drying characteristics of pore networks

Somkiat Prachayawarakorn [a,*], Preeda Prakotmak [b], Somchart Soponronnarit [b]

[a] Faculty of Engineering, King Mongkut's University of Technology Thonburi, Suksawat 48 Road, Bangkok 10140, Thailand
[b] School of Energy and Materials, King Mongkut's University of Technology Thonburi, Suksawat 48 Road, Bangkok 10140, Thailand

Received 6 March 2006
Available online 20 September 2007

Abstract

Simulation of isothermal drying using two-dimensional networks comprised of interconnected cylindrical pores is presented. Transport of moisture inside pore segments was described by Fick's law. The results have shown that the shielding of large pores by the smaller pores in the stochastic pore network, which is supposed to be representative of real porous medium, causes the lower drying rate and hence lower effective diffusion coefficient as compared to those predicted from the idealized network of pores with a single size. The strength of shielding is found to vary with the characteristics of pore size distribution as interpreted by the moisture concentration experienced by the pores, which is remarkably different amongst the pore size distributions. The inefficient transport of moisture through the stochastic pore network can be improved or even better with the suitable architecturally assembled structure. The minimum shielding archetype network, appearing very high porous at particle surface, is predicted to enhance greatly the drying rate. On the other hand, the maximum shielding network, which is small pores allocated onto the network exterior, exhibits the slowest drying rate.
© 2007 Elsevier Ltd. All rights reserved.

Keywords: Drying; Effective diffusion coefficient; Stochastic pore network

1. Introduction

Drying of porous materials has received much attention in a number of industrial applications including wood [1], pharmaceutical product [2], foodstuffs [3], and paper [4]. While material is dried, moisture inside the material transports through its interfacial void spaces to the surface and is carried away to the flowing stream. The transport of moisture may be occurred by several mechanisms of mass transfer, such as Knudsen diffusion, molecular diffusion, capillary flow, etc. All the drying mechanisms are lumped into the effective (apparent) diffusion coefficient [5–7] and the porous material is considered as a continuum. This consideration leads to formulation of partial differential equations which relate to the changes of quantities, i.e. temperature and moisture content with time. By using the continuum models, the effective diffusion coefficient can experimentally be determined from the drying characteristic curve. The value of the effective diffusion coefficient varies from material to material although the drying conditions used, i.e. temperature and superficial air velocity, are all the same. The summary of the effective diffusion coefficients for products are given by [8]. However, the interpretation of those results have ignored the pore structural issues and relied on empirical representations. Such empiricisms may not be useful for providing detailed information on how moisture diffuses through void spaces, with different sizes and shapes, which dictate the diffusive pathways of moisture.

Thus, it is desirable to obtain the structural models that are capable of taking into accounts key geometrical and topological properties such as dead ends and variations in pore size and tortuous trajectories. When the structural model is combined with the transport equations, the flow

* Corresponding author. Tel.: +662 4270 9221; fax: +662 428 3534.
E-mail address: somkiat.pra@kmutt.ac.th (S. Prachayawarakorn).

0017-9310/$ - see front matter © 2007 Elsevier Ltd. All rights reserved.
doi:10.1016/j.ijheatmasstransfer.2007.03.055

Nomenclature

C	moisture content (decimal dry basis)
$\overline{C}$	average moisture content (decimal dry basis)
D	diffusion coefficient (m^2/s)
Fo	Fourier number, $\frac{D\Delta t}{\Delta x^2}$
N	drying rate, kg water/s, or number of pores in network
Pr	probability distribution function
L	material thickness (m)
l	pore length (m)
r	pore radius (m)
t	drying time (s)
x	distance along the pore length (m)

Greek symbols

σ	standard deviation (m)
μ	mean pore radius (m)
Γ	gamma function
κ	adjustable parameter of uniform distribution
ψ	adjustable parameter of uniform distribution
α	adjustable parameter of bimodal distribution
β	adjustable parameter of bimodal distribution

Subscripts

e	equilibrium
eff	effective

of substances through pore segments inside porous solid can numerically be predicted [9–11] and hence the effective properties are calculated, thereby providing the understanding of macroscopic properties. In such a way, network models can be used in the modeling of transport processes such as single-phase and two-phase fluid flow and pore diffusion [12–15].

In this work, the drying of the random or stochastic pore network, which is supposed to be representative of pore spaces of real porous particle, is investigated. The moisture movement inside the pore segments is described by Fick's law and the drying process occurs under isothermal condition. The effect of pore size distributions on the drying characteristic curve and subsequent effective diffusivity is theoretically determined. In addition to the pore size distribution, the geometrical configuration of the pores, which is a full set of pores assembled in different ways onto the network, is explored how the diffusion of moisture through such geometrical structure exhibits different to that predicted from the stochastic pore network. This geometrical structure, sometimes called as pore architecture in this work, has similar pore size distribution to that employed in the stochastic pore network.

2. Network model

Fig. 1 shows an example of scanning electron micrograph (SEM) views of dried durian chip obtained from the freeze and hot air dryings. Pores shown in Fig. 1 are represented by black color and tissue by grey color. Porosity of the material appears to consist of a randomised assembly of pore spaces, which are more or less randomly interconnected. As shown from the figure, different drying techniques can produce remarkably different microstructures. Durian chip dried by the freeze-drying technique is more porous and larger pore sizes than that dried by hot air. With the hot air dried sample, the dense layer is formed and the small pores appear at the surface.

To understand the transport of moisture through the pore spaces, the pore sizes of the real solid is mapped onto an array of lattices (shown in 2-D in Fig. 2). Each pore in the real solid becomes a bond in one of the lattices and each pore junction becomes a node. In this study, the pore shape assigned onto the network is assumed to be cylindrical geometry and all pores in the network are assumed to have

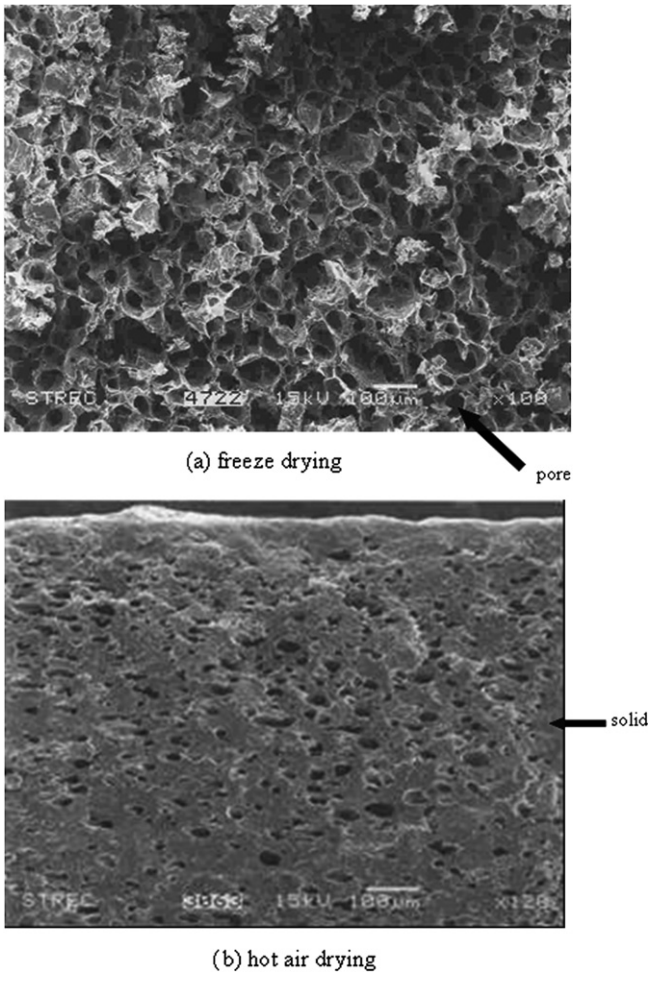

(a) freeze drying

(b) hot air drying

Fig. 1. SEM images of durian chip obtained from different drying techniques.

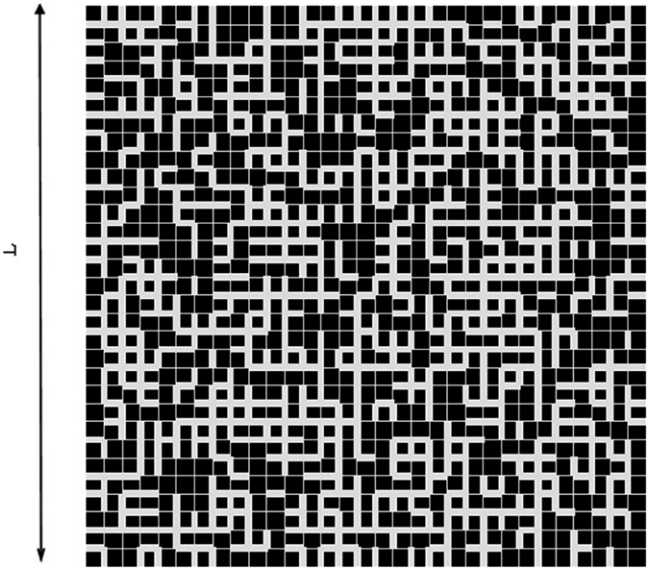

Fig. 2. 2-D 30 × 30 random pore network.

the same length. The pores with different sizes are randomly placed onto the network and this approach provides pore at any positions within the network independent to the neighboring pores. Fig. 2 illustrates 2-D pore network with a size of 30 × 30, consisting of 1860 pores. Each pore junction has a connectivity of 4. Real pore sizes of solid, which may determined by nitrogen adsorption or mercury porosimetry, are assigned to the bonds so that the real structure and the network model have the same pore size distribution. Let L is the average particle size of material. The length of each pore, l, is then calculated by dividing L by $N+1$, where N is the network size. Moisture leaves from the network via all the pores at the network periphery, which open onto the drying medium.

2.1. Diffusion in single pores

When the pore network is established, the diffusion problem is solved by calculating the moisture content inside the individual pore in conjunction with the mass balance of moisture at the pore junctions. It is assumed that the moisture diffusing through pore with radius $r_{i,j}$, occurs under isothermal condition. The isothermal condition occurs when heat required for evaporation balances with heat from conduction and convection. The change of moisture inside individual pores of the network is described by the following equation:

$$\frac{\partial C}{\partial t} = D\frac{\partial^2 C}{\partial x^2} \tag{1}$$

where C is the moisture content (decimal dry basis), D the diffusion coefficient (m^2/s), t the drying time (s) and x the distance along the pore length (m). The diffusion coefficient is assumed to be a constant value and the moisture concentration in the pores at the beginning is specially uniform along the pore axis. To determine the moisture profile along the length, the forward finite difference is applied and Eq. (1) is thus expressed as

$$C^{p+1}_{m,r_{i,j}} = Fo\left(C^{p}_{m-1,r_{i,j}} + C^{p}_{m+1,r_{i,j}}\right) + (1-2Fo)C^{p}_{m,r_{i,j}} \tag{2}$$

where Fo is the Fourier number, $Fo = \frac{D\Delta t}{\Delta x^2}$, p and m the respective indexes of the present drying time and of nodal position along the pore. Eq. (2) is stable when Fo ranges between 0 and 0.5. The transfer rate $N_{i,j}$ of moisture, for any time t, diffusing into a pore with radius of $r_{i,j}$ can be calculated by

$$N_{r_{i,j}} = \pi r^2_{i,j} D\left(\frac{\mathrm{d}C_{r_{i,j}}(x,t)}{\mathrm{d}x}\right)_{x=l}. \tag{3}$$

2.2. Mass balance in the network

After drying starts, the pore ends positioned at the exterior network are exposed to the drying medium and have moisture equal to equilibrium moisture content, assuming negligible convective mass transfer resistance. This assumption allows the moisture contents of the exterior pores at any drying time to be calculated directly. For the interior pores, the calculation of their moisture contents is not straightforward since the moisture contents at the two ends of pore is not known. To determine the internal moisture contents, the mass balance of moisture content at inner nodes of the network is made, assuming the size of pore junctions being zero and no accumulation at the pore junctions within the network. The sum of all in and outflows, for a small time interval, at any node is accordingly zero. That is,

$$\sum_{j\in\{i\}} N_{r_{i,j}} = 0 \tag{4}$$

where $\{i\}$ refers to the set of i-adjacent nodes which are connected to node (i) in the network. By solving the moisture in every node together the specified boundary conditions around the network periphery, the average moisture content $\overline{C}_{\text{network}}$ of the network can readily be calculated. The calculation, based on the volume average, can be expressed by

$$\overline{C}(t)_{\text{network}} = \frac{\sum_{n=1}^{N} r^2_{i,j}\int_0^l C_{r_{i,j}}(x,t)\,\mathrm{d}x}{N\cdot l\sum_{n=1}^{N} r^2_{i,j}} \tag{5}$$

where N is the number of pore in the network and l is the pore length (m).

2.3. Effective diffusivity

If the diffusion is occurring through the slab-shaped porous solids, the effective diffusivity can be determined by Fick's second law of diffusion, which is expressed by

$$\frac{\overline{C}(t)-C_e}{C_i-C_e} = \frac{8}{\pi^2}\sum_{n=0}^{\infty}\frac{1}{(2n+1)^2}\exp\left[-(2n+1)^2\frac{\pi^2 D_{\text{eff}}t}{L^2}\right] \tag{6}$$

where $\overline{C}(t)$ is the average moisture content of material (decimal dry basis), C_i the initial moisture content, C_e the equilibrium moisture content, D_{eff} the effective diffusion coefficient and L the material thickness. Eq. (6) presents the diffusion of moisture in one direction. The drying of pore network at the present study is, however, occurred in two directions and the solution is obtained from the product of the above diffusion equation itself, thus eventually yielding

$$\frac{\overline{C}(t)-C_e}{C_i-C_e}=\left(\frac{8}{\pi^2}\right)^2\left[\exp\left(-2\pi^2\frac{D_{eff}\times t}{L^2}\right)+\left(\frac{2}{9}\right)\exp\left(-10\pi^2\frac{D_{eff}\times t}{L^2}\right)+\left(\frac{2}{25}\right)\exp\left(-26\pi^2\frac{D_{eff}\times t}{L^2}\right)+\cdots\right] \quad (7)$$

The first three terms of infinite series of Eq. (7) are employed to quantify the effective diffusivity and a trial-error method is used. The effective diffusivity is obtained when the difference between the value of moisture content predicted by Eq. (7), $\overline{C}(t)$, and that calculated from the network, $\overline{C}(t)_{network}$, is less than the acceptable value. By this method, the evolution of moisture content at pore level directly reflects on the effective diffusivity.

2.4. Pore size distribution

Pore size distribution defined in the range from a minimum to a maximum pore radius, r_{min} and r_{max}, is described in terms of the number diameter probability density function which is given by

$$f(r)=\frac{d\left(\frac{N(r)}{N_T}\right)}{dr}, \quad r_{min}<r<r_{max} \quad (8)$$

where N_T is the total pores in the network and $N(r)$ presents the number of pores between r and $r+dr$. The integration of Eq. (8) from r_{min} to r_{max} equals to unity, $\int_{r_{min}}^{r_{max}} f(r)\,dr=1$. The probability distribution function of all pores in the network with radius larger than a particular radius, $Pr(r_i)$, is

$$Pr(r_i)=\int_{r_i}^{r_{max}} f(r)\,dr \quad (9)$$

The values of $Pr(r_i=r_{min})=1$ and of $Pr(r_i=r_{max})=0$. In this study, the following three types of pore size distribution, i.e. normal distribution, uniform distribution and bimodal distribution were used:

Normal size distribution:

$$f(r)=\frac{1}{\sigma\sqrt{2\pi}}\exp\left(-\frac{1}{2}\left[\frac{r-\mu}{\sigma}\right]\right), \quad -\infty<r<\infty \quad (10)$$

Uniform size distribution:

$$f(r)=\frac{1}{\kappa-\psi}, \quad \psi\leqslant r\leqslant\kappa \quad (11)$$

Bimodal size distribution:

$$f(r)=\frac{r^{\alpha_1-1}}{\Gamma(\alpha_1)\beta_1^{\alpha_1}}\exp\left(-\frac{r}{\beta_1}\right)+\frac{r^{\alpha_2-1}}{\Gamma(\alpha_2)\beta_2^{\alpha_1}}\exp\left(-\frac{r}{\beta_2}\right), \quad 0\leqslant r\leqslant\infty \quad (12)$$

where σ is the standard deviation, μ the mean pore radius, $\Gamma(\alpha)$ the gamma function and κ, ψ and α all the adjustable parameter.

Before investigating the diffusive flow behaviour within the network of pores, pore sizes are generated by the mapping of a sequence of uniformly distributed numbers in the range of 0 and 1 on the corresponding probability distribution function $Pr(r_i)$ and then are randomly distributed to the bonds.

3. Results and discussion

Drying simulations were performed on the pore network model. At the beginning, every pore within the network is assumed to have equal moisture content, with the value of 0.35 dry basis. When the drying starts, moisture content at the periphery pores immediately equilibrates to the surrounding air, which is assumed to be 0.165 dry basis in this study. The diffusivity value used in the simulations was 1×10^{-10} m^2/s. To minimize the effect of periphery pores on the transport of moisture, size of the network should sufficiently be large. In addition, it enables to capture the moisture transport inside the large network closed to that occurring inside the real porous materials, consisting of many thousands of pores. A network size of 45×45, consisting of 4140 pores in the network, was used in this study. For each set of results reported, 20–30 realisations were carried out and the average value was presented.

3.1. Influence of pore size distribution width

Pore size distribution is the important parameter not only in quality of foods but also in transport of moisture [16]. Their structures are given by a nature or through processing. To simplify the problem, this work assumes that the structure of foods does not change with time. Two case studies were performed; the first deals with the width of pore size distribution and the latter deals with the influence of characteristics of pore size distribution (see Section 3.2).

In the first case, the simulations were performed with the normal size distribution to determine the effect of pore size distribution width on the average moisture content. The width of distribution can be made by varying the value of standard deviation. A mean pore radius was given, with a size of 40 μm. The average moisture contents of the networks versus time are plotted in Fig. 3 for the values of standard deviation (σ) of 1, 7, and 12 μm. The moisture content of the network, for a given standard deviation, is rapidly decreased at the early drying period and slowly decreased afterwards. This trend is generally found in drying curve of porous materials.

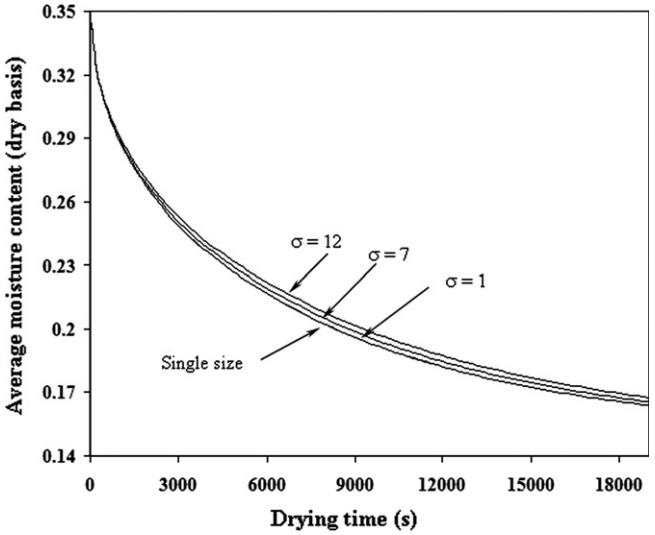

Fig. 3. Influence of pore size distribution width on moisture content (normal size distribution with $\mu = 40$ μm).

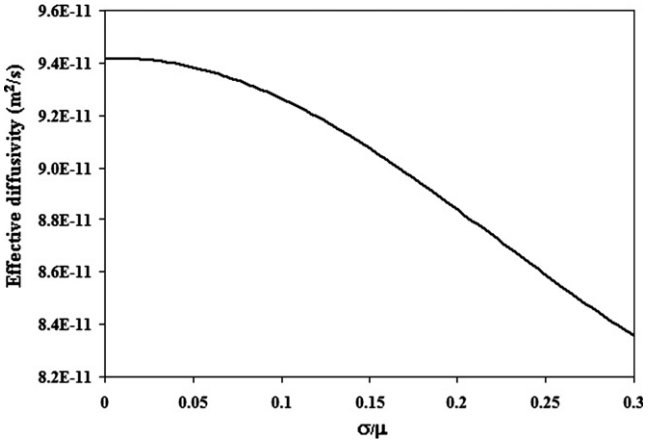

Fig. 4. Influence of pore size distribution width on transport property ($\mu = 40$ μm).

As shown in Fig. 3, difference in drying rate amongst pore size distribution widths is clearly evident after which moisture content of the networks is reduced below 0.25 dry basis. The moisture content is reduced faster with the narrower pore size distribution, corresponding to smaller standard deviation. When the standard deviation becomes unity, the decrease of moisture content is almost identical to that of the network of single-sized pore. The single-sized network is an ideal network where the moisture diffusing through any pore in the network is not interfered by their adjacent pores. These simulation results emphasize the less efficient transport of moisture within the network consisting of large and small pores, which are randomly connected. The poor transport is due to the larger pores shifted behind smaller ones and this effect is named as pore "shielding" [17]. Such shielding results in the moisture existing in the shielded pores difficult to move from the interior to the exterior because of the strong diffusional resistances in the surrounding pores.

However, the pore shielding effect is insignificant at the early drying period since the main portion of moisture removed at this time is present near the network periphery in which the moisture movement is not interfered by the disorder of void spaces within the network. Thus, the reduction of moisture content with time is nearly the same for the networks of pores that possess different standard deviations of pore size, as shown in Fig. 3.

The influence of the pore size distribution width on the drying curve presented in Fig. 3 is similar to that reported by Metzger and Tsotsas [18], exhibiting the strong effect of standard deviation of pore sizes on the drying behaviour. In their model, voids in porous material were represented as cylindrical shape and their arrangement was in parallel direction to fluid flow. The parallel capillaries were connected all along their length with no any resistance and fluid present in the capillaries was transported by the capillary and viscous forces. However, Segura and Toledo [19], who studied the isothermal drying of pore networks by assuming the dominant contribution of capillary forces over the viscous forces, reported the opposite results to the above studies. In their work, the simulation showed an insignificant effect of pore size distribution on the drying curves of the pore networks.

Fig. 4 shows the influence of width of pore size distribution on the effective diffusivity with a mean value of 40 μm. The effective diffusivity of the network reduces as the value of σ/μ increases. The value of effective diffusivity decreases from 9.4×10^{-11} m^2/s at the σ/μ of zero to 8.3×10^{-11} m^2/s at the σ/μ of 0.3. These results respond to the similar way found in the drying curves, showing the faster drying rate with lower value of standard deviation.

3.2. Influence of type of pore size distribution

In this section, the change in moisture transport, while it diffuses through the network with different distributive pores, i.e. uniform, normal and bimodal distribution, is studied. In comparison, the networks of pores, which are characterized by different types of pore size distribution, have equal total pore volume and the network length is equal. The structural parameters required to generate pore size distributions are given as follows:

Normal size distribution: $\mu = 40$ μm and $\sigma = 10$ μm
Uniform distribution: $\kappa = 74.13$ μm and $\psi = 4.97$ μm
Bimodal distribution: $\beta_1 = 3$ μm, $\beta_2 = 10$ μm, $\alpha_1 = 2$ μm and $\alpha_2 = 4.9$ μm

For the single-sized network, which is used as a baseline, the pore size of 40 μm was employed. Fig. 5 shows the number diameter probability density function of pores generated from different types of pore size distributions using the above structural parameters. In the bimodal distribution, the pore sizes are generally characterized by two groups, small and large pores. Pore sizes produced from

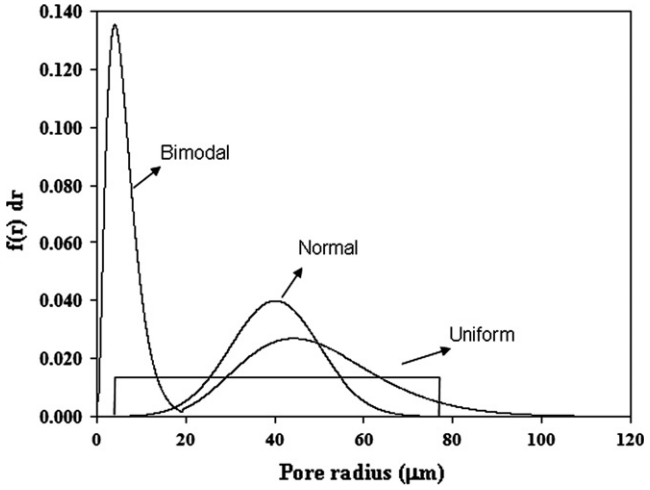

Fig. 5. Number diameter probability density function generated from different types of pore size distribution under the same total pore volume.

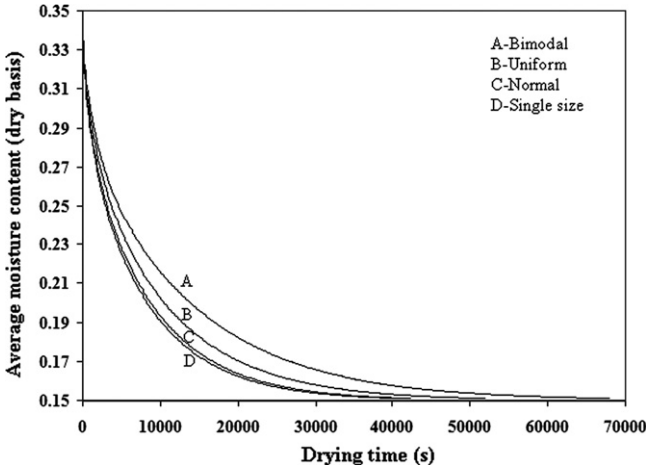

Fig. 6. Influence of type of pore size distribution on moisture content.

the structural bimodal parameters were given in the range of small pores from 0.34 to 17.3 μm, accounting for 36% of total number of pores allocated onto the network, and in the range of large from 17.3 to 121.8 μm, accounting for 64% of total number of pores. For the uniform distribution, the generated pore sizes ranged between 1.9 and 71 μm.

Fig. 6 shows the influence of type of pore size distribution on reduction in moisture content, indicating the strong impact of pore size distribution on the moisture change.

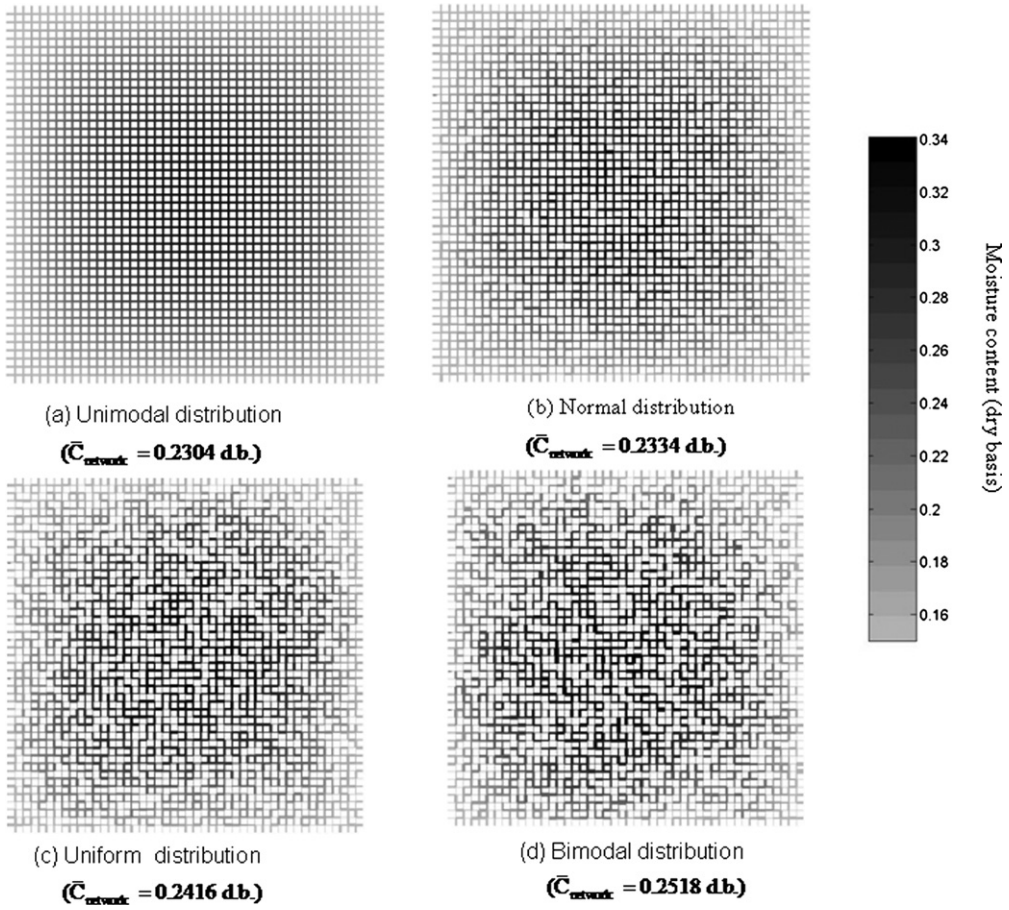

Fig. 7. Moisture content in 2-D pore networks with different distributions of pore sizes.

The rate of moisture reduction is lowest with the bimodal distribution and it becomes faster with the following uniform and normal distributions. Moreover, the fastest rate of moisture reduction exhibits in the single-sized network for which the shielded pores are absent. The moisture transport through the bimodal network is least efficient in spite of the larger pore sizes and higher pore volume in the large pore assembly, both of which normally serve high flow of moisture because of low resistance of moisture diffusion in the large pores. However, the slowest drying rate for the bimodal pores can be attributed to the fact that the large pore assembly ineffectively communicates itself throughout the network and some of them possibly allocate behind the smaller pores. Thus, the moisture diffusion from the inside to the outside for this pore size distribution is strictly limited. This description can be interpreted through the representation of network moisture gradients in voids which will be shown in Fig. 7.

The changes of average moisture content of the networks, with different pore size distributions, shown in Fig. 6 are selected for a particular drying time of 4500 s to visualize the moisture content of each pore positioned within the networks. The pictorialized representations of local moisture content are shown in Fig. 7. Each pore was colored according its moisture content. The representative colors with 21 shades from light grey to black were used for the corresponding range of moisture content from less than 0.16–0.34 dry basis. After drying is passed, difference in the detailed moisture contents amongst the networks of pores is shown up. As shown in Fig. 7d for the "bimodal" network, the inefficient connection of large and small pore assemblies exhibits the delay of moisture in percolating through the network once the drying front approaches the smaller pores. Irregular pattern of moisture content is also found with the bimodally distributed pores.

The results from the simulations also indicate that the moisture at the innermost pores of the "bimodal" network for the illustrative drying time of 4500 s is the same content as at the initial one (black), implying that drying at that area does not commences. With the other networks, the moisture at the innermost had already decreased, reducing from 0.34 to 0.32 dry basis which corresponds to the dark grey color.

3.3. Effect of structure re-ordering on the drying kinetics

The food materials in particular fruit possess dense physical structure and sugar content. When it is conventionally dried, the crust or dense layer may possibly be formed near the material surface. This created structure does not facilitate internal moisture movement, thus resulting in long drying time, browning and darkening of product and large energy consumption. One approach to improve the drying rate is to change its physical structure, for example, making it more porous. This can be made by the foaming of fruit before drying [20]. In this section, the concept of pore network is utilised to show how the drying rate can be changed when the physical structure of material is modified. Two illustrative structures are given to show the scope for this.

The first structure is shown in Fig. 8a whereby the full set of random pores, generated from the normal distribution ($\sigma = 10$ μm and $\mu = 40$ μm), is assembled in rank order and then spirally wound into positions in the network, with the largest pore at the exterior and the smallest at the centre. This architectural structure, namely minimum shielding network, exhibits very more porous at the exterior

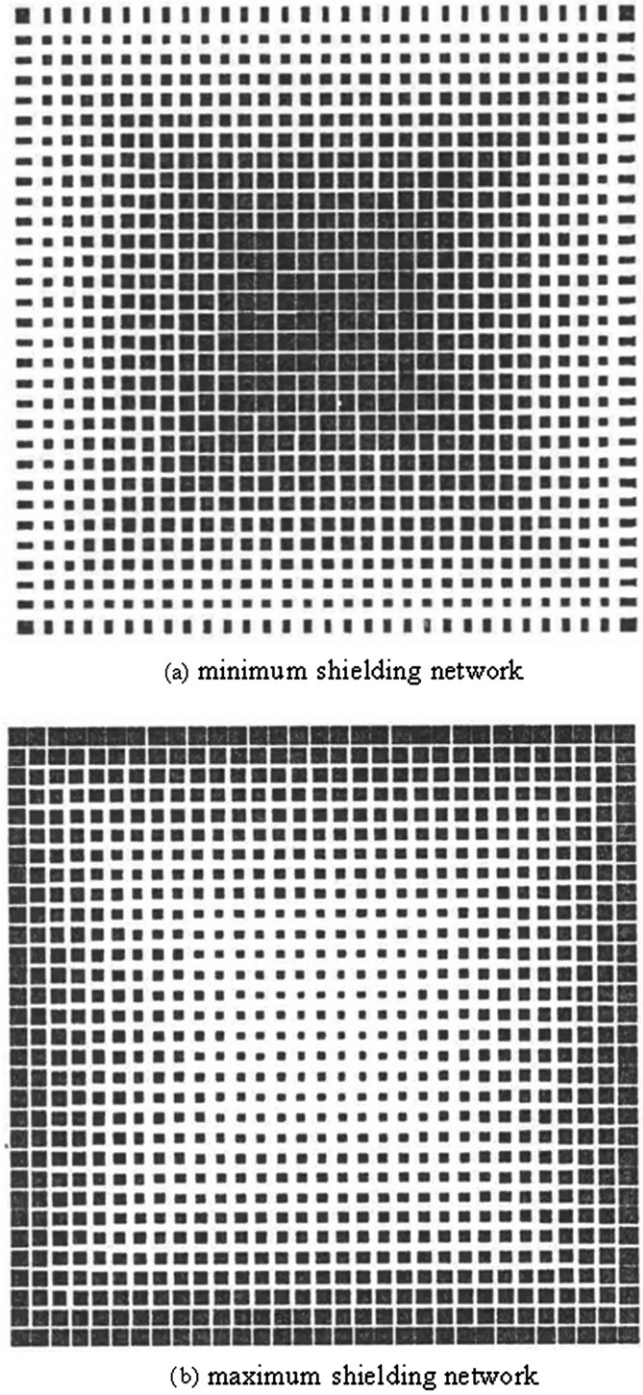

Fig. 8. Illustrative pore architectural structures.

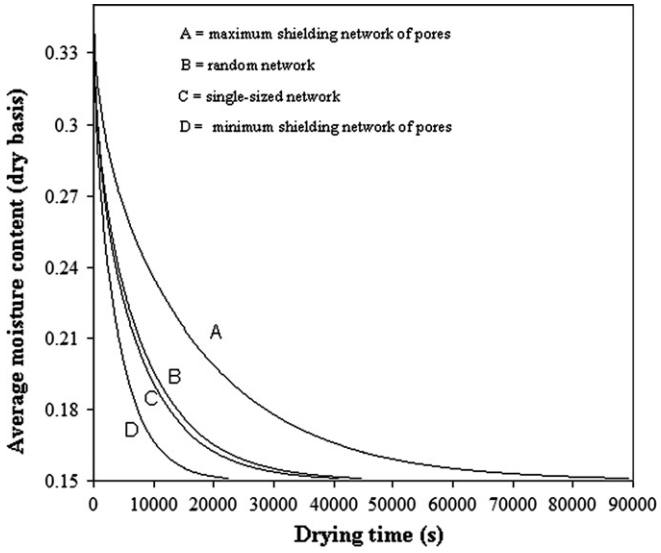

Fig. 9. Effect of pore architectural structure on the drying kinetics.

surface as shown in Fig. 8a. On the other hand, if the pores are allocated into the network, with the smallest size at the exterior surface and the largest at the centre, it can be visualized as a dense layer at the surface, which is shown in Fig. 8b, which is named as maximum shielding network. The outer dense layer of the later pore structure may possibly be similar to that occurring in the biomaterials containing high sugar content when dried with hot air. Both pore structures shown in Fig. 8 have exactly identical pore sizes used in the stochastic pore network. The simulation results obtained from the above archetypal pore structures are shown in Fig. 9. The transport of moisture through different configurations of pore assembly is strikingly different. The reduction of moisture content is very fast with the pore structure appearing very porous at the exterior (D) and extremely slowest with the dense structure at the exterior (A). The corresponding effective diffusivities are 1.57×10^{-10} m^2/s and 3.81×10^{-11} m^2/s.

The moisture content of each pore for the architectural configurations is shown in Fig. 10, for the illustrative drying time of 4500 s which is the same time as presented in Fig. 7. As shown in Fig. 10a for the minimum shielding network, the moisture content of the exterior pores at that time lies in between 0.16 and 0.2 dry basis, corresponding to the shade of grey color which increases intensity from light to medium grey. This result implies the architectural pore structure with very high porous at the outer surface facilitating the high diffusive flux of moisture, thereby enhancing the rapid fall in moisture content.

Because of high resistance of moisture diffusion in the small pores at the periphery for the maximum shielding network, the diffusion of moisture is restricted and this is clearly evident from Fig. 8b, showing the grey color shade only at the periphery pores whilst most inner pores have moisture contents above 0.3 dry basis.

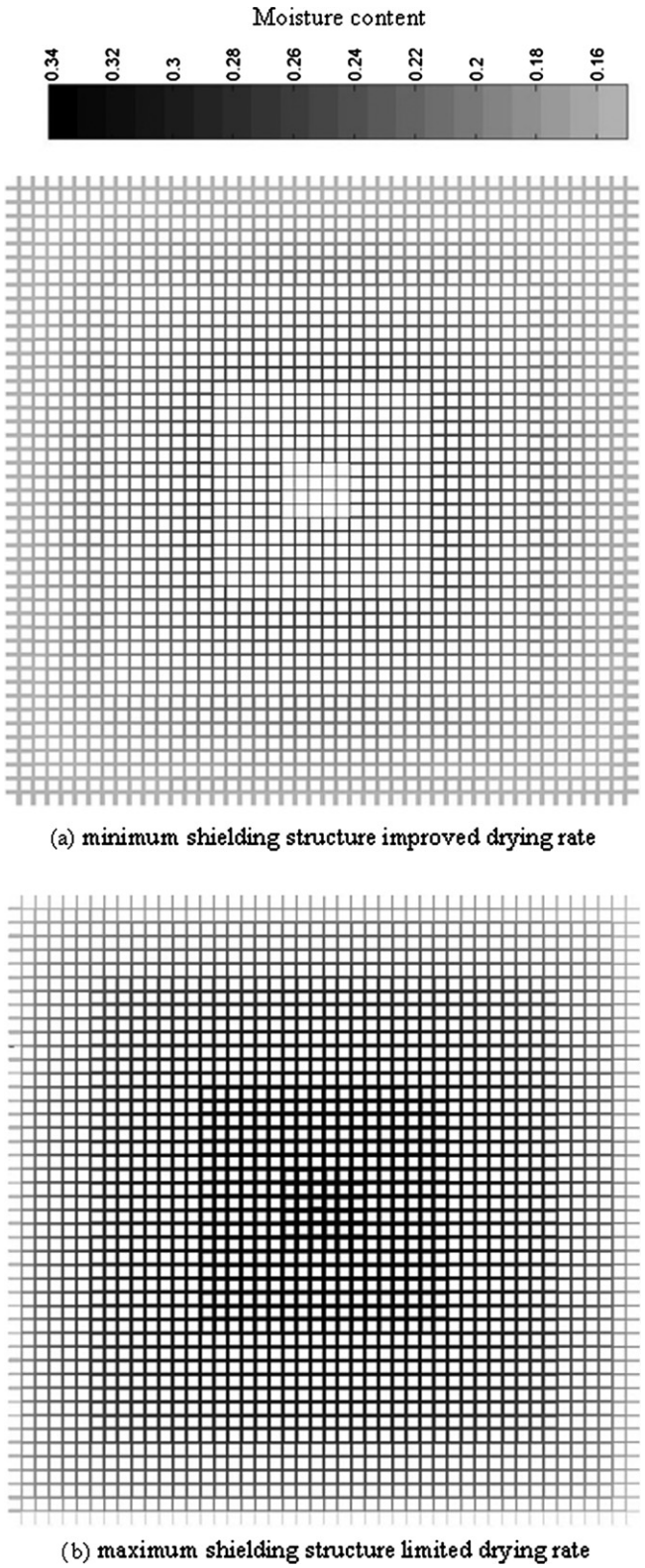

Fig. 10. Moisture content in 2-D network with different arrangements of pore assembly.

4. Conclusions

A 2-D pore network for the drying of moisture content under isothermal condition has been studied. The transport

of moisture within individual pore segments is described by Fick's second law. The simulation results have been shown that the effect of shielding inherent in typical random pore network results in slower decrease of moisture content and hence lower value of effective diffusion coefficient as compared to the single sized network for which the shielding is absent. Degree of shielding is different among pore size distributions and this effect causes the value of effective diffusion coefficient to be dependent on the distribution types. The strongest shielding effect is found with the pore network characterized by bimodal pore size distribution and this influence consequently results in drying of bidisperse porous structure relatively longer time than the other illustrative pore size distributions, i.e. uniform and normal distribution. The drying rate of the stochastic pore network can be improved through the proper pore structure. This superiority is greatest with the network of pores appearing highly porous at the exterior. On the other hand, porous particles, with a dense layer at the surface or consisting of small exterior pores, can be dried with lowest rate.

Acknowledgements

The authors express their sincere appreciation to the Thailand Research Fund and commission on higher education for financial support.

References

[1] D. Elustondo, S. Avramidis, S. Shida, Predicting thermal efficiency in timber radio frequency vacuum drying, Dry. Technol. 22 (2004) 795–807.
[2] K.H. Gan, R. Bruttini, O.K. Crosser, A.I. Liapis, Freeze-drying of pharmaceuticals in vials on trays: effects of drying chamber wall temperature and tray side on lyophilization performance, Int. J. Heat Mass Transfer 48 (2005) 1675–1687.
[3] L.A. Campañone, V.O. Salvadori, R.H. Mascheroni, Food freezing with simultaneous surface dehydration: approximate prediction of freezing time, Int. J. Heat Mass Transfer 48 (2005) 1205–1213.
[4] J. Seyed-Yagoobi, H. Noboa, Drying of uncoated paper with gas-fired infrared emitters – optimum emitters' location within a paper machine drying section, Dry. Technol. 21 (2003) 1897–1908.
[5] G. Efremov, T. Kudra, Calculation of the effective diffusion coefficients by applying a quasi-stationary equation for drying kinetics, Dry. Technol. 22 (2004) 2273–2279.
[6] Md. Raisul Islam, J.C. Ho, A.S. Mujumdar, Convective drying with time-varying heat input: simulation results, Dry. Technol. 21 (2003) 1333–1356.
[7] S. Prachayawarakorn, P. Prachayawasin, S. Soponronnarit, Effective diffusivity and kinetics of urease inactivation and color change during processing of soybeans with superheated-steam fluidized bed, Dry. Technol. 22 (2004) 2095–2118.
[8] N.P. Zogzas, Z.B. Maroulis, D. Marinos-Kouris, Moisture diffusivity data compilation in foodstuffs, Dry. Technol. 14 (1996) 2225–2253.
[9] M. Blunt, Flow in porous media-pore – network models and multiphase flow, Curr. Opin. Colloid Interface Sci. 6 (2001) 197–207.
[10] R. Mann, Development in chemical reaction engineering: issues relating to particle pore structures and porous materials, Trans. IchemE 71A (1993) 551–561.
[11] M. Sahimi, G.R. Gavalas, T.T. Tsotsis, Statistical and continuum models of fluid–solid reactions in porous media, Chem. Eng. Sci. 45 (1990) 1442–1502.
[12] S.C. Nowicki, H.T. Davis, L.E. Scriven, Microscopic determination of transport parameters in drying porous media, Dry. Technol. 10 (1992) 925–946.
[13] J.B. Laurindo, M. Prat, Numerical and experimental network study of evaporation in capillary porous meida. Drying rates, Chem. Eng. Sci. 53 (1998) 2257–2269.
[14] M. Prat, Isothermal drying of non-hygroscopic capillary-porous materials as an inversion percolation process, J. Multiphase Flow 21 (1995) 875–892.
[15] V.G. Mata, J.C.B. Lopes, M.M. Dias, Porous media characterization using mercury porosimetry simulation. 1. Description of the simulator and its sensitivity to model parameters, Ind. Eng. Chem. Res. 40 (2001) 3511–3522.
[16] M.S. Rahman, O. Al-Amri, I.M. Al-Bulushi, Pores and physico-chemical characteristics of dried tuna produced by different methods of drying, J. Food Eng. 53 (2002) 301–313.
[17] G.P. Androutsopoulos, R. Mann, Evaluation of mercury porosimeter experiments using a network pore structure model, Chem. Eng. Sci. 34 (1979) 1203–1212.
[18] T. Metzger, E. Tsotsas, Influence of pore size distribution on drying kinetics: a simple capillary model, Dry. Technol. 23 (2005) 1797–1809.
[19] L. Segura, P.G. Toledo, Pore-level modeling of isothermal drying of pore networks: effects of gravity and pore shape and size distributions on saturation and transport parameters, Chem. Eng. J. 111 (2005) 237–252.
[20] C.K. Sanket, F. Castaigne, Foaming and drying behaviour of ripe bananas, Lebensm-Wiss. Univ. Technol. 37 (2004) 517–525.

In press in An International Journal of Drying Technology

Modeling of Diffusion with Shrinkage and Quality Investigation of Banana Foam Mat Drying

Ratiya Thuwapanichayanan[1,*], Somkiat Prachayawarakorn[2] and Somchart Soponronnarit[1]

[1]School of Energy, Environment and Materials, [2]Faculty of Engineering

King Mongkut's University of Technology Thonburi

126 Pracha u-tid Road, Bangkok 10140, Thailand

ABSTRACT

A diffusion model including shrinkage has been developed for predicting the change of moisture content in banana foam mats during drying. Two solution methods, moving boundary using variable grid and immobilizing boundary using the Lagrangian referential coordinate, were used in exploring their capabilities to predict the moisture change. Banana foam mats with initial foam densities of 0.3, 0.5 and 0.7 g/cm^3 were dried at 60, 70 and 80°C and superficial air velocity of 0.5 m/s. The qualities of the final products in terms of texture and microstructure were determined. The moving boundary method can predict the moisture content more accurate than the immobilizing boundary method especially in the case of low density foam. The quality determinations showed that the initial foam density strongly affected hardness, crispness and morphology of dried banana foam mats whilst the drying temperature had no significant effect on those qualities.

Keywords diffusion model; immobilizing boundary; moisture diffusivity; moving boundary

* Correspondence: Ratiya Thuwapanichayanan, School of Energy, Environment and Materials, King Mongkut's University of Technology Thonburi, 126 Pracha u-tid Road, Bangkok 10140, Thailand; E-mail: t_ratiya@yahoo.com

INTRODUCTION

Banana is fast perishable after harvesting. Dehydration of banana can provide an extension of shelf-life and also reduce losses. Banana chip, one of the most favorite products, can be served as a snack food or added in cereal breakfast. The combination of foaming and hot air drying is an alternative method to produce banana chips.

Banana foam initially consists of gas bubbles and aqueous phase. When moisture in banana foam starts vaporization, porous structure appears. The creation of a porous structure can improve the textural properties of dry crisp foods in particular hardness and crispness. In addition, banana foam can be rapidly dried to 0.04 kg/kg db, which is a desired value for the crisp products [1]. Study of the drying process of banana foam is therefore important for producing crisp banana chips with desired quality. Design of efficient drying conditions can improve the product quality as well as reduce the energy consumption. Mathematical models are useful tools for pre-design that can reduce the trial and error efforts involved in experimentation.

The mathematical formulation of mass transfer in porous material during drying is often based on a Fick's second law. The moisture movement inside porous media can occur in forms of liquid and vapor [2]. Liquid diffusion, capillary flow and surface diffusion can take place in liquid phase. Molecular diffusion and Knudsen diffusion are possible mechanisms for vapor transport. These mechanisms are lumped into an effective diffusivity. In principle, the effective diffusivity can be determined experimentally. For the materials undergoing shrinkage, variations in volume must be considered in the effective diffusivity [3,4].

In case of banana foam, shrinkage is very severe because instability of gas bubbles yields bubble collapse, in addition to stresses-induced shrinkage. Shrinkage of material results in a shorter distance for the moisture travelling from inside to the

outside. Shrinkage effect should therefore be taken into account in the diffusion model, in order to successfully describe the transport of moisture inside the samples.

Several solution methods can be used for solving the diffusion model including shrinkage such as immobilizing boundary using the Lagrangian referential coordinate [3,4,5,6] and moving boundary using variable grid [7]. The latter method is more realistic to allow for changes in the dimensions. However, it is more complex as compared to the first method.

The objective of this work was therefore to evaluate the capability of two solution methods, moving boundary and immobilizing boundary, in predicting the moisture content in banana foam mats during drying. The important qualities of the final products, i.e. texture and microstructure were also reported.

MATERIALS AND METHODS

Preparation of banana puree and foam

Gros Michel bananas (*Musa Sapientum* L.) at a mature stage of 5, which contained total soluble solids of approximately 23-25ºBrix, were used. Bananas were cut into slices with a slicing machine. To prevent discoloration during foaming, the sliced bananas were pretreated by immersing them in 1% (w/w) sodium metabisulphite solution for 2 min and then rinsed with distilled water for 30 sec [8]. The pretreated banana slices were chopped into small pieces and then blended with a blender (Waring, model no. 8011 BU, Torrington, CT) for 1 min. About 800 g of the banana puree was then poured into a mixing bowl and 5% fresh egg albumen (on a wet puree basis) used as the foaming agent was added to the banana puree. The banana puree with egg albumen was whipped by a Kitchen Aid Mixer (model no. 5K5SS, Strombeek-Bever, Belgium) at a maximum speed to foam densities of 0.3, 0.5 and 0.7 g/cm^3.

Foam density was determined by measuring the mass of a fixed volume of the foam. Determination was performed carefully to avoid destroying the foam structure and to ensure that there were no voids while filling the foam into the measuring beaker. The experiments were done in duplicate.

The moisture content of the foamed banana is normally determined by the vacuum oven method 934.06 [9]. However, drying of foamed banana in a hot air oven at a temperature of 103ºC for 3 hr was used instead of AOAC method [9]. The moisture content determined by the hot air oven was closed to that obtained by the vacuum oven method, the percentage error from two methods approximately 0.4%.

Drying procedure

Banana foam mats with a thickness of 5 mm were placed on a mesh tray, which was covered with aluminum foil, and then put into the drying chamber. The samples at three foam densities of 0.3, 0.5 and 0.7 g/cm^3 were then dried to about 0.03 kg/kg db using the drying air temperatures of 60, 70 and 80°C and a superficial air velocity of 0.5 m/s. Moisture loss from the samples was determined by weighing the sample tray outside the drying chamber using an electronic balance (±0.01 g).

Texture analysis

Banana foam mats, after drying to about 0.03 kg/kg db, were taken to examine their textural properties. The texture of dried banana foam mats was evaluated by a compressive test using a texture analyzer model TA.XT.plus (Stable Micro Systems, Surrey, UK). The sample was placed on the hollow planar base. The test applied a direct force to the sample using a 5 mm spherical probe at a constant crosshead speed of 2 mm/s. The hardness was defined as the maximum force of the force-deformation curve and the crispness was characterized by the number of peaks and the slope of the first peak. Eight samples were tested and the average values of hardness and crispness were presented.

Microstructural analysis

A scanning electron microscope (JEOL JSM-5600LV, Tokyo, Japan) was used to characterize the microstructure of dried banana foam mats. The dried banana foam mat was placed on two-side adhesive tape attached to metal stub and was coated with gold. SEM micrographs were taken at an accelerating voltage of 10 kV and a magnification of 35×.

MATHEMATICAL MODEL

A Fick's diffusion model was used to describe the transport of moisture inside a single banana foam mat. The main assumptions used in the proposed model were that the product shape was an infinite slab, the moisture transfer and volume change took place only in the thickness direction. In addition, the external resistance to moisture transfer was negligible and the moisture distribution inside banana foam before drying was spatially uniform. The moisture diffusion inside banana foam can be expressed by the following equation [10]:

$$\frac{\partial M}{\partial t} = \frac{\partial}{\partial x}\left(D_v^{eff} \frac{\partial M}{\partial x} \right), 0<x<L(t) \quad (1)$$

where D_v^{eff} is the effective moisture diffusivity (m^2/s), L(t) is the sample thickness varying with the moisture content (m), M is the local moisture content (kg/kg d.b.), x is the coordinate along the diffusion path and t is the drying time (s).

Since the effective moisture diffusivity is not constant, the space derivative of the product of D_v^{eff} and $\frac{\partial M}{\partial x}$ on the right side of Eq. (1) can then be written as:

$$\frac{\partial M}{\partial t} = D_v^{eff} \frac{\partial^2 M}{\partial x^2} + \frac{\partial M}{\partial x}\frac{\partial D_v^{eff}}{\partial x}, 0<x<L(t) \quad (2)$$

SOLUTION METHODS

Two solution methods, moving boundary and immobilizing boundary, are presented for solving a diffusion model including shrinkage for banana foam mat. The two solution methods have been extensively used for shrinkage problem, however, slight modifications of both methods are needed for banana foam.

Moving boundary

Moving boundary is a method in which the domain of integration (x) is not constant. The variable grid central finite difference was used and the spacing between each grid point (Δx_i) was not equal and not constant. The number of grid points (Fig. 1) was kept constant during the time steps of calculation.

The values of moisture content at each grid point were solved from the nonlinear partial differential equation (Eq. (2)), together with the earlier mentioned assumptions. Eq. (2) was discretized in the positions by the variable grid central finite difference method in its explicit form as follows:

$$\frac{M_i^{j+1} - M_i^j}{\Delta t} = D_{v,i}^{eff,j} \frac{\frac{M_{i+1}^j - M_i^j}{\Delta x_{i+1}^j} - \frac{M_i^j - M_{i-1}^j}{\Delta x_i^j}}{\frac{\Delta x_{i+1}^j}{2} + \frac{\Delta x_i^j}{2}} + \frac{M_{i+1}^j - M_{i-1}^j}{\Delta x_{i+1}^j + \Delta x_i^j} \cdot \frac{D_{v,i+1}^{eff,j} - D_{v,i-1}^{eff,j}}{\Delta x_{i+1}^j + \Delta x_i^j} \quad (3)$$

where subscript i and superscript j represent node and time indexes, respectively.

As the moisture content at each grid point was known, the spacing between each grid point was then adjusted according to the average moisture content of each section. From the experiments, it was found that a decrease in the thickness of banana foam mats was in a linear relation with the moisture content, which could be described by the following equation:

$$L/L_0 = a+bM/M_0 \quad (4)$$

where a is 0.349, 0.496 and 0.503, b is 0.702, 0.521 and 0.507 for the initial foam densities of 0.3, 0.5 and 0.7 g/cm^3, respectively. L is the thickness of banana foam mat at a given moisture content (m), L_0 is the thickness of banana foam mat at the beginning (m) and M_0 is the initial moisture content of banana foam mat (kg/kg d.b.).

In this work, it was assumed that the relationship between spacing of each section and average moisture content in that section was in a linear function. It can be calculated by applying Eq. (4) for differential element and it can be written as:

$$\Delta x_i / \Delta x_0 = a + b(M_{av} / M_0) \quad (5)$$

where Δx_i is the spacing between each grid point (m), Δx_0 is the spacing between grid point at the beginning (m), M_{av} is the average moisture content of each section (kg/kg d.b.), M_0 is the initial moisture content at the beginning (kg/kg d.b.).

As the spacing between each grid point was adjusted, the thickness of banana foam mat was also updated; the sum of the new spacing of each section was the new thickness of banana foam mat. The average moisture content of banana foam mat at each time step was then calculated by integration of the local moisture content over the new thickness of banana foam mat. This calculation procedure was repeated until the desired final moisture content was achieved.

Immobilizing boundary

Immobilizing boundary is a method for solving shrinkage problems, in which the domain of integration of the diffusion equation is constant. In order to fix the domain of integration, the Lagrangian coordinate (ξ,t) was used instead of the Eulerian coordinate (x,t).

Considering many foodstuffs, i.e., potato, fish fillet and banana, it was assumed that no pores or air voids are present and these products consist of solid (dry matter) with volume V_s and liquid (water) with volume V_w. The variation of the material volume during drying is equal to the volume of evaporated water whilst V_s remains constant throughout the drying time. The volume of solid is thus chosen as the Lagrangian referential coordinate (ξ) for such system in order to fix the domain of

integration. The maximum value of ξ is the thickness of the dry product (zero moisture content) if the diffusion and the shrinkage are assumed to be unidirectional.

The Lagrangian coordinate and the Eulerian coordinate are related by the mass of the solid (m_s) [6,11] and it can be expressed by:

$$\rho_s A dx = \rho_s^{\xi} A d\xi \tag{6}$$

where A is surface area (m^2), ρ_s is the apparent density of the solid (kg/m^3), which is the ratio between the mass of the solid and its overall volume, and ρ_s^{ξ} is the apparent dry solid density (kg/m^3), which is the ratio between the mass of the solid and the volume of the dry product.

Rewriting Eq. (6), it is thus obtained:

$$\frac{\partial \xi}{\partial x} = \frac{\rho_s}{\rho_s^{\xi}} \tag{7}$$

The transformation of Eq. (1) into the Lagrangian coordinate can be obtained by using Eq. (7) and it can be expressed as:

$$\frac{\partial M}{\partial t} = \frac{\partial}{\partial \xi}\left(D_v^{eff} \left(\frac{\rho_s}{\rho_s^{\xi}} \right)^2 \frac{\partial M}{\partial \xi} \right), \; 0 < \xi < L_f \tag{8}$$

where L_f is the thickness of the dry product (m).

In case of the banana foam, its overall volume initially consists of volume of solid (V_s), volume of water (V_w) and volume of air voids (V_a) which were produced during the whipping process and not occupied by water. We have to determine the Lagrangian referential coordinate which is similar to the bi-constituent systems (solid and liquid) as described earlier, that is, the coordinate, which was chosen as the Lagrangian referential, must be constant during water diffusion. If the volume of the dry banana foam mat, which consisted of volumes of solid and air voids, was considered as the Lagrangian referential coordinate, both volumes remained constant throughout the drying time.

When the volumes of solid and air voids were fixed, the sample shrinkage occurred solely due to the moisture loss. The maximum value of ξ was the thickness of dry banana foam mat since the diffusion and the shrinkage were assumed to be one-dimension.

The relationship between ρ_s and ρ_s^{ξ} is given by:

$$\frac{\rho_s}{\rho_s^{\xi}} = \frac{V_f}{V} = \frac{L_f}{L} \tag{9}$$

Because the diameter of banana foam mat was constant, the volume change of banana foam mat occurred only in the thickness. V_f/V is then equal to L_f/L where V is the volume of banana foam mat at a given time (m^3) and V_f is the volume which was chosen as the Lagrangian referential coordinate.

The ratio of L_f and L can be derived from Eq. (4). Since a in Eq. (4) is the y-intercept which is equal to L_f/L_0, so that Eq. (4) can be rearranged in form of L_f/L as:

$$L_f / L = \frac{1}{1 + \frac{b}{a}(M / M_0)} \tag{10}$$

where $\frac{b}{a}$ is called as the shrinkage coefficient (β).

Substituting Eq. (10) into Eq. (8), it yields:

$$\frac{\partial M}{\partial t} = \frac{\partial}{\partial \xi}\left(D_v^{eff} \frac{1}{\left(1 + \beta(M / M_0)\right)^2} \frac{\partial M}{\partial \xi} \right), \; 0 < \xi < L_f \tag{11}$$

Eq. (11) was discretized in the positions by the central finite difference method in its explicit form and it can be expressed as:

$$\frac{M_i^{j+1}-M_i^j}{\Delta t}=\frac{D_{v,i}^{eff,j}}{\left(1+\beta\frac{M_i^j}{M_0}\right)^2}\cdot\frac{\left(M_{i+1}^j-2M_i^j+M_{i-1}^j\right)}{(\Delta\xi)^2}+\frac{1}{\left(1+\beta\frac{M_i^j}{M_0}\right)^2}\cdot\frac{\left(M_{i+1}^j-M_{i-1}^j\right)\left(D_{v,i+1}^{eff,j}-D_{v,i-1}^{eff,j}\right)}{4(\Delta\xi)^2}$$
$$-\frac{2\beta D_{v,i}^{eff,j}}{M_0\left(1+\beta\frac{M_i^j}{M_0}\right)^3}\cdot\frac{\left(M_{i+1}^j-M_{i-1}^j\right)^2}{4(\Delta\xi)^2} \quad (12)$$

As the local moisture content was known, the average moisture content of banana foam mat at each time step was then calculated by integration of the local moisture content over the thickness of the dry banana foam mat.

The R-square (R^2) and root mean square error (RMSE) were used to estimate the accuracy of average moisture content prediction. The RMSE was calculated as follows:

$$RMSE=\sqrt{\frac{\sum_{i=1}^{N}\left(Y_{exp,i}-Y_{pre,i}\right)^2}{N}} \quad (13)$$

where $Y_{exp,i}$ and $Y_{pre,i}$ are respectively the experimental and predicted average moisture content of banana foam mats at a given time (kg/kg db) and N is the number of average moisture content measurements.

RESULTS AND DISCUSSION

Effective moisture diffusivity

The effective diffusivity of banana foam mats determined by the method of slopes is shown in Fig. 2 (a-b). The detail of calculation can be seen from Karathanos [12]. The effective diffusivity decreased with decreasing moisture content, except for the early stage of drying where the effective diffusivity increased with decreasing moisture content due to the rapid rise of product temperature. In addition to the moisture content, the effective moisture diffusivity was higher when the drying temperature increased and the initial foam density decreased.

The relationship between effective moisture diffusivity and average moisture content of banana foam is described by the following empirical equation:

$$D_{eff}(M) = a \exp\left(\sum_{i=1}^{4} \alpha_i M^i\right) \quad (14)$$

where a and α_i are the empirical parameters. The a and α_i depended on the initial foam density and drying temperature and were obtained by non-linear regression analysis; the results together with R^2 values are presented in Table 1. The proposed equation could adequately describe their relationship with R^2 values being in the range of 0.945-0.998.

Model validation

Fig. 3 (a-c) shows the comparisons between experimental data and predictions of average moisture content of banana foam mats at different initial foam densities. It could be observed that the accuracy of predictions of the average moisture content throughout the drying time were different amongst the calculation methods, moving and immobilizing boundaries. The moving boundary method could predict the experimental results more accurate than the immobilizing boundary method especially for the case of

low initial foam densities. At initial foam density of 0.3 g/cm^3 and drying temperature of 80°C, R-square values (R^2) were 0.98 and 0.49 and root mean square error values (RMSE) were 0.14 and 0.66 for moving and immobilizing boundary methods, respectively. This is attributed to the simplified assumption of the immobilizing boundary method, that is, the volume of air voids presented in a banana foam mat remained constant throughout the drying time. As the volume of air voids was assumed to be fixed, the sample shrinkage occurred only due to the moisture loss. Nevertheless, the shrinkage of banana foam mats at initial foam density of 0.3 g/cm^3 did not follow this assumption. At this foam density, the reduced volume was larger than the volume of removed water (the data was not shown here) due to the collapse of gas bubbles which occurred during the non-rigid state of the foam.

When the immobilizing boundary method was applied to the higher initial foam densities, 0.5 and 0.7 g/cm^3. The predictions of average moisture content of banana foam mats by this method approached to those predicted by the moving boundary method as shown in Fig. 3 (b-c), resulting in higher values of R^2 and lower values of RMSE as presented in Table 2. This is because the shrinkage of banana foam mats at higher initial foam densities was nearly equal to the volume of evaporated water. In addition, the predictions by immobilizing boundary method are satisfactory for high density foods, i.e., potato, fish fillets and purified chitosan [3,4,5,6].

The time required for reducing the moisture content of banana foam mats to about 0.03 kg/kg db was lesser when using lower initial foam densities (Fig. 3) due to the larger air voids which were produced at lower foam density (see SEM micrographs). A larger amount of water could easily travel through the larger voids, resulting in shorter drying time. As shown in Fig. 4, the drying time was also shorter when the banana foam mats were dried at higher drying temperature due to the higher moisture diffusivity. The

difference between experimental and simulated drying time when using the moving boundary method was within 6% in all cases.

Fig. 5 shows the comparisons between experimental data and predictions of thickness change of banana foam mats at different initial foam densities. It can be seen that the moving boundary method could predict the sample shrinkage corresponding to the experimental data. As depicted in Fig. 5, the samples at low initial foam density were more shrunk than those at higher initial foam densities.

Quality of dried banana foam mats

Fig. 6 (a-d) shows SEM micrographs of banana foam mats dried at different temperatures for various initial foam densities. It was observed that the pore shape of dried banana foam mats was elongate whilst the pore shape of banana foams before drying was spherical (not shown here). This is probably due to the stress formation during drying, which led to some distortion.

For the textural properties, it was found that hardness and crispness were strongly affected by their microstructures. The samples with initial foam density of 0.3 g/cm^3, in which adhesive-forces between solid matrices were not strong, yielded the lesser dense structure and lower strength. Hence, the hardness was smaller as compared with that of the samples with higher initial foam densities (see Fig. 7a). In terms of crispness, the samples with lower initial foam densities had smaller number of peaks and lower slopes of the first peak as shown in Fig. 7 (b-c). The small number of peaks and low initial slope obtained from samples at low initial foam density of 0.3 g/cm^3 indicated that this banana foam was less crisp as compared with the samples at higher initial foam densities. The hardness and crispness of samples dried at higher or lower temperatures were not different because the morphology of these samples was

insignificantly different as previously shown in Fig. 6. However, the hardness and crispness of samples with initial foam density of 0.7 g/cm^3 and dried at 60°C were not reported since their moisture content could not be reduced to the desired value, approximately 0.04 kg/kg db, at which the products were not crisp [1].

CONCLUSIONS

The diffusion model including shrinkage solved by moving boundary method could predict the average moisture content more accurate than the immobilizing boundary method. The initial foam density strongly affected the moisture diffusivity where the lower foam density, corresponding to the larger voids, provided higher values of effective diffusivity and resulted in shorter drying time. Moreover, the initial foam density affected the morphology and textural properties of dried banana foam mats whilst the drying temperature had no significant effect on those qualities. The extensive porous structure of banana foam at lower densities led to lower values of hardness and crispness.

ACKNOWLEDGEMENTS

The authors express their appreciation to the Thailand Research Fund (TRF) and the Commission on Higher Education for the financial supports.

REFERENCES

1. Matz, S.A. *Snack Food Technology*; The AVI Publishing Company: Westport, 1976.
2. Waananen, K.M.; Litchfield, J.B.; Okos, M.R. Classification of drying models for porous solids. Drying Technology **1993**, *11*(1), 1-40.
3. Pinto, L.A.A.; Tobinaga, S. Diffusive model with shrinkage in the thin-layer drying of fish muscles. Drying Technology **2006**, *24*, 509-516.
4. Batista, L.M.; da Rosa, C.A.; Pinto, L.A.A. Diffusive model with variable effective diffusivity considering shrinkage in thin layer drying of chitosan. Journal of Food Engineering **2007**, *81*, 127-132.
5. Rovedo, C.O.; Suarez, C.; Viollaz, P.E. Drying simulation of a solid slab with three dimensional shrinkage. Drying Technology **1995**, *13*(1&2), 371-393.
6. Chemkhi, S.; Zagrouba, F.; Bellagi, A. Modelling and simulation of drying phenomena with rheological behaviour. Brazilian Journal of Chemical Engineering **2005**, *22*(2), 153-163.
7. Balaban, M. Effect of volume change in foods on the temperature and moisture content predictions of simultaneous heat and moisture transfer models. Journal of Food Process Engineering **1989**, *12*, 67-88.
8. Krokida, M.K.; Kiranoudis, C.T.; Maroulis, Z.B.; Marinos, D. Effect of pretreatment on color of dehydrated products. Drying Technology **2000**, *18*(6), 1239-1250.
9. AOAC. *Official Methods of Analysis* (16^{th} ed.); AOAC International: Washington, D.C., 1995.
10. Crank, J. *The Mathematics of Diffusion*; Clarendon Press: Oxford,1975.

11. Gekas, V.; Lamberg, I. Determination of diffusion coefficients in volume changing systems-application in the case of potato drying. Journal of Food Engineering **1991**, *14*, 317-326.
12. Karathanos, V.T.; Villalobos, G.; Saravacos, G.D. Comparison of two methods of estimation of the effective moisture diffusivity from drying data. Journal of Food Science **1990**, *55*(1), 218-223.

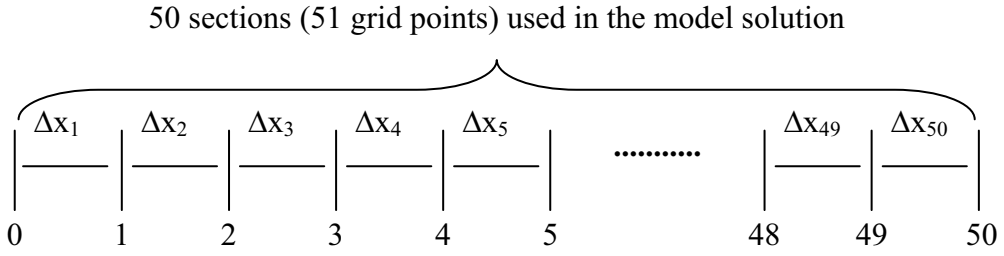

FIG. 1. Finite difference grid points (point 0 is the bottom and point 50 is the surface)

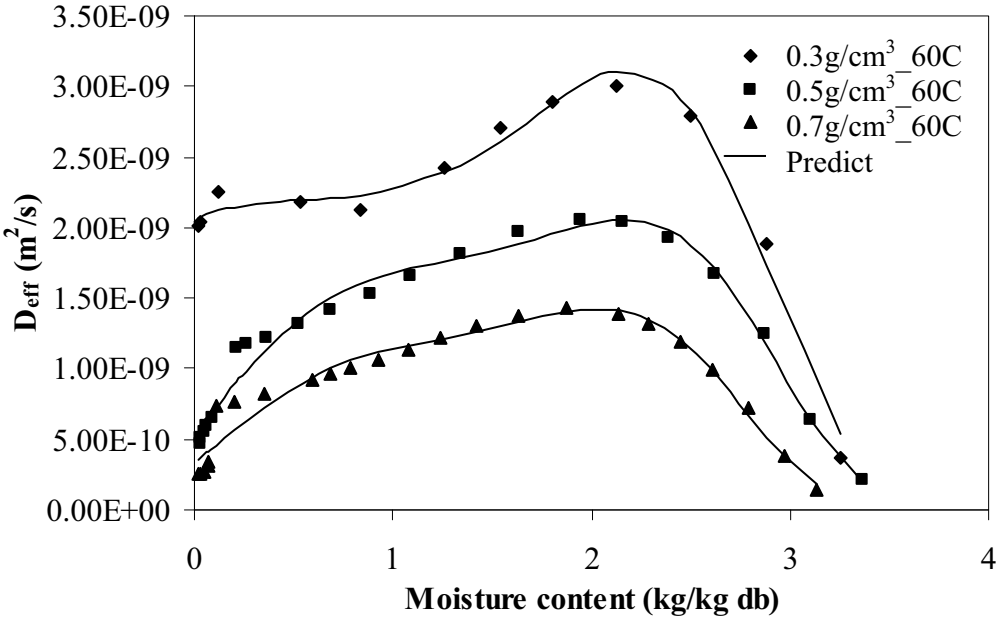

(a)

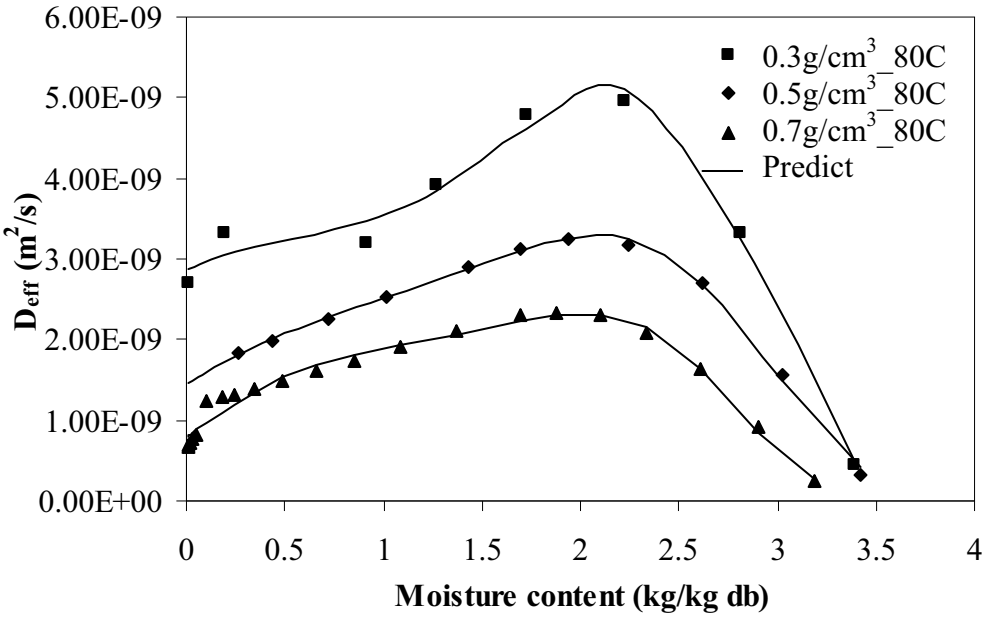

(b)

FIG. 2. Moisture diffusivity of banana foam mats at different drying conditions

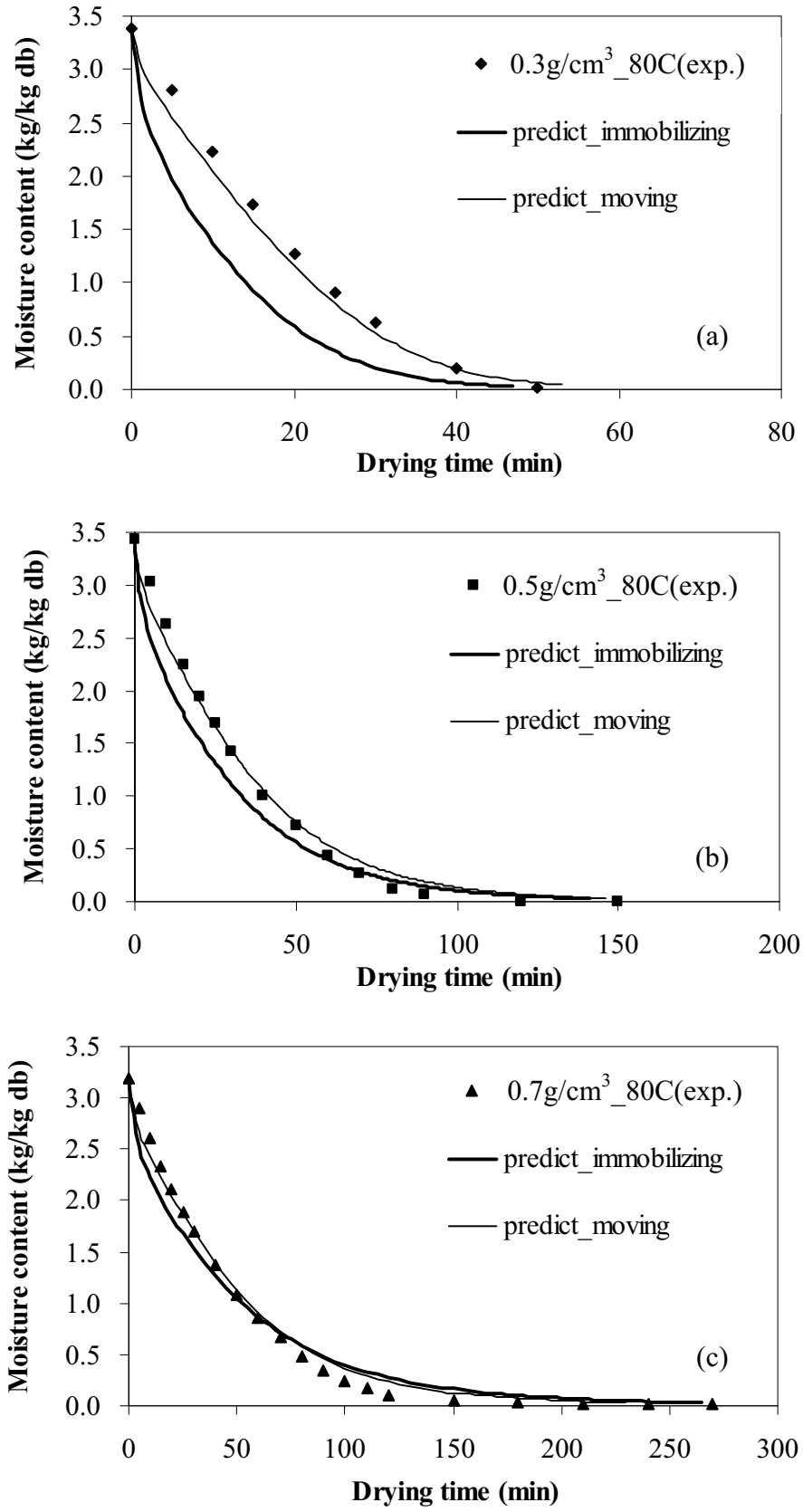

FIG. 3. The comparison between experimental data and predictions of average moisture content of banana foam mats at different initial foam densities

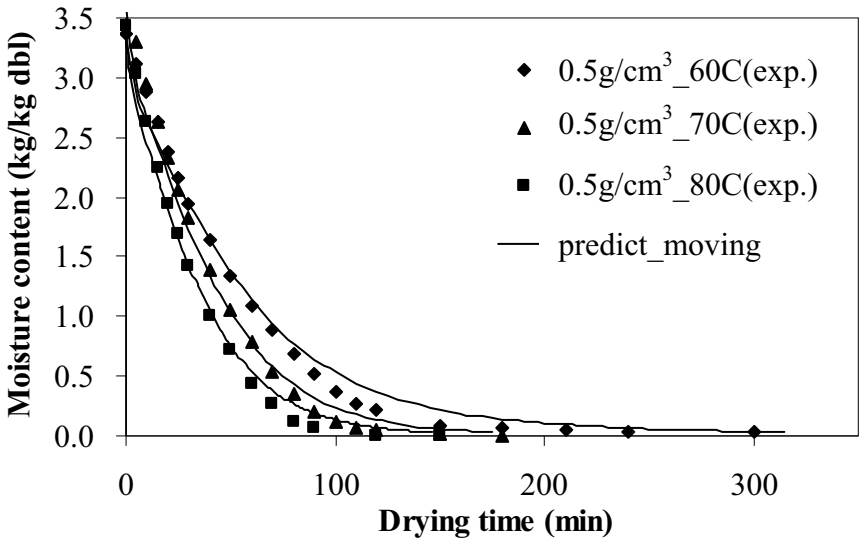

FIG. 4. The comparison between experimental data and predictions of average moisture content of banana foam mats at different drying temperatures

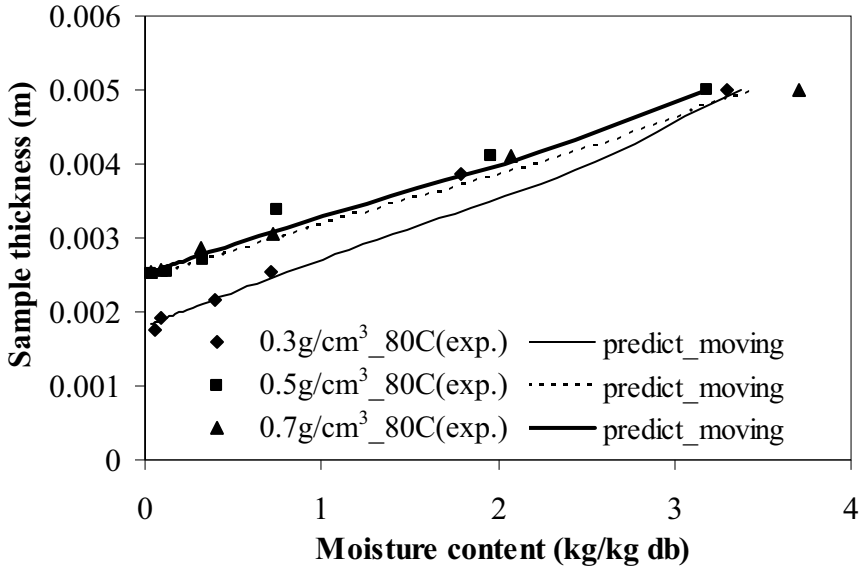

FIG. 5. The comparison between experimental data and predictions of thickness changes of banana foam mats at different drying conditions

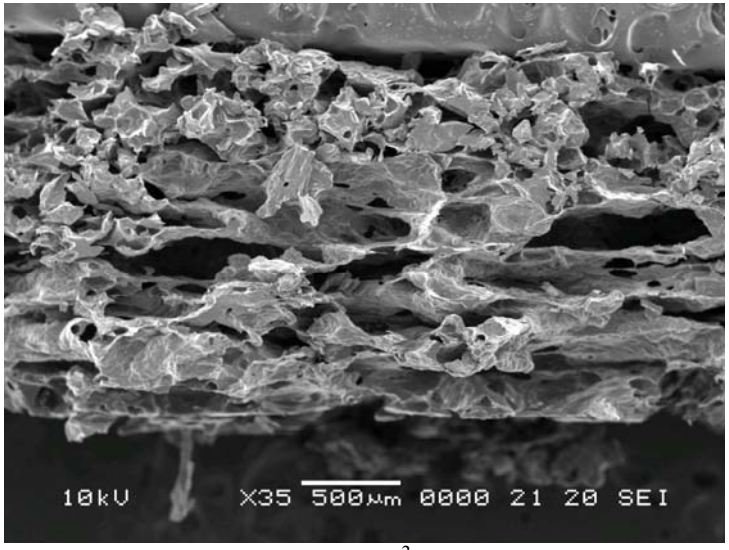

(a) 0.3 g/cm^3, 60°C

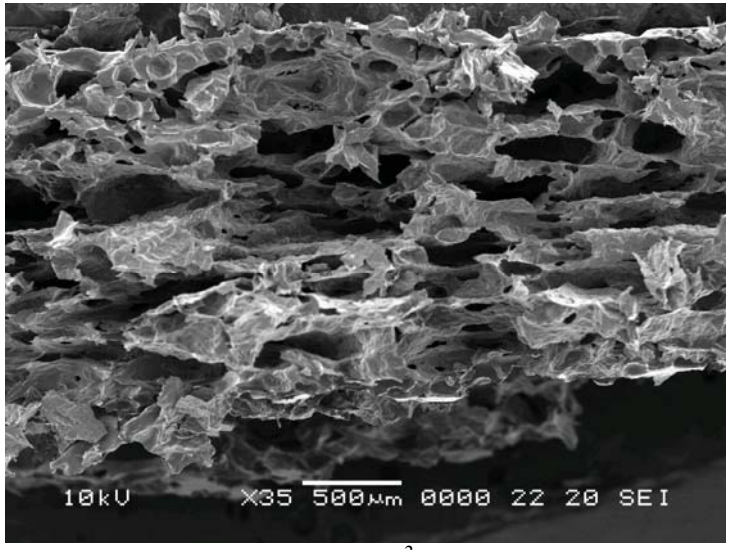

(b) 0.3 g/cm^3, 80°C

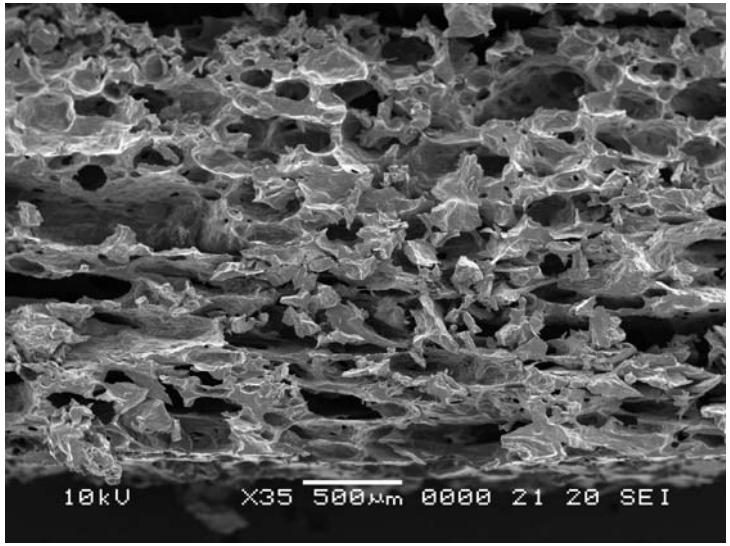

(c) 0.5 g/cm^3, 60°C

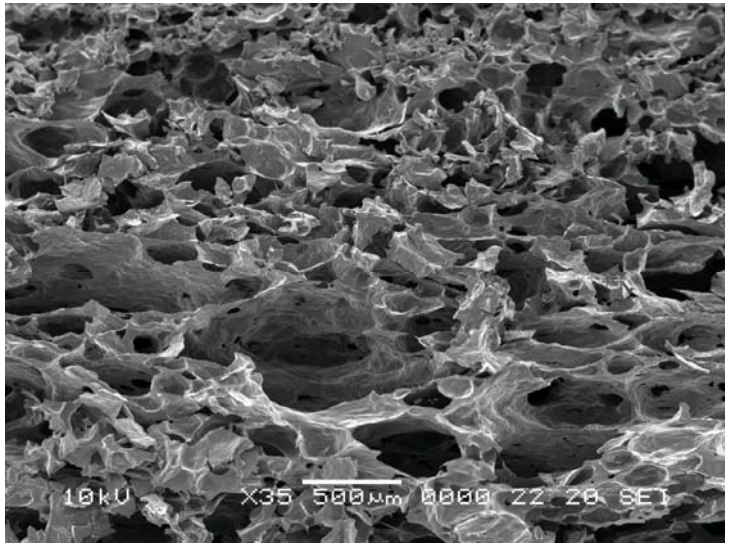

(d) 0.5 g/cm^3, 80°C

FIG. 6. (a-d) SEM micrographs of dried banana foam mats at different initial foam densities and drying temperatures

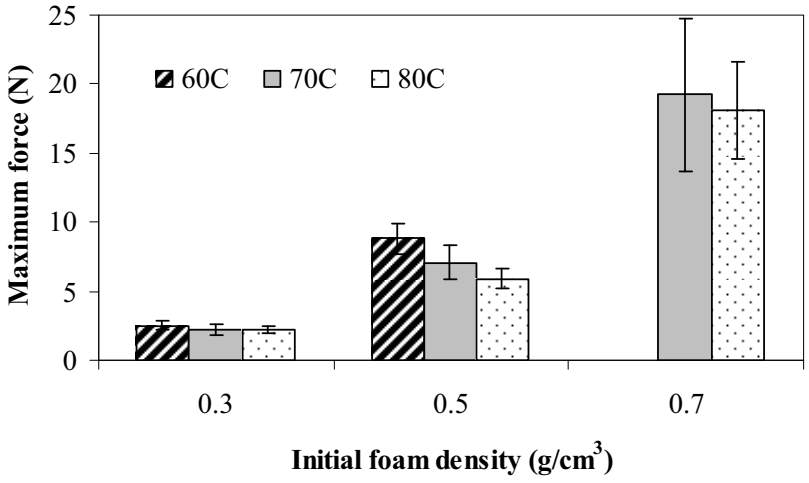

(a)

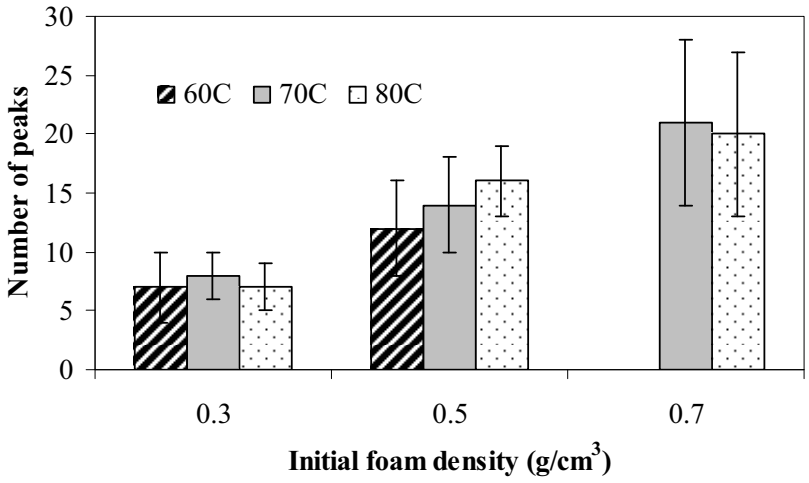

(b)

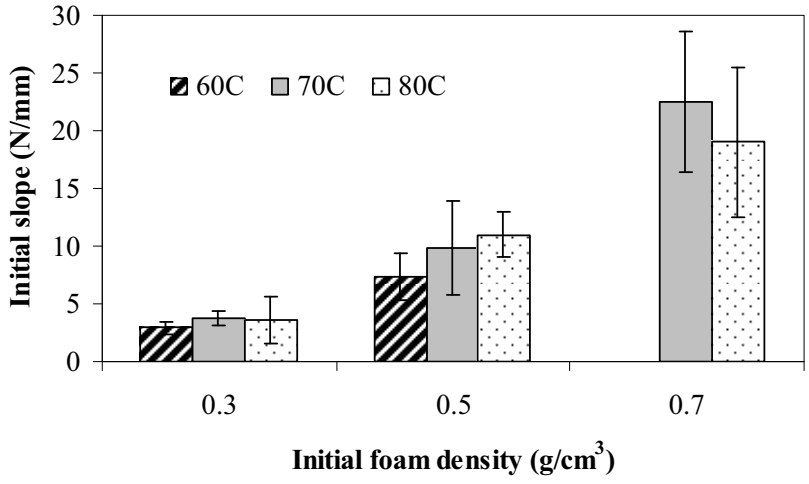

(c)

FIG. 7. Effects of initial foam densities and drying temperatures on (a) Maximum force, (b) Number of peaks and (c) Initial slope of dried banana foam mat

TABLE 1

The calculated values of a and α_i (Eq. (14)) for various foam densities and drying temperatures

Drying condition		Empirical parameter					
Foam density (g/cm^3)	Temperature (°C)	$a\times10^{-10}$	α_1	α_2	α_3	α_4	R^2
0.3	60	20.4978	0.3823	-0.750	0.6042	-0.138	0.980
	70	25.4514	0.5247	-1.013	0.7768	-0.177	0.964
	80	28.5214	0.4324	-0.602	0.5060	-0.121	0.983
0.5	60	5.5042	2.8784	-2.8579	1.3158	-0.2218	0.974
	70	12.9837	0.8666	-0.6938	0.3734	-0.0763	0.998
	80	14.5071	1.0528	-0.8794	0.476	-0.099	0.996
0.7	60	3.3549	3.1578	-3.2075	1.5468	-0.2762	0.953
	70	4.4478	3.7392	-4.0588	1.9792	-0.3497	0.945
	80	7.879	2.2188	-2.2754	1.1498	-0.2157	0.973

TABLE 2

The R-square values (R^2) and root mean square error values (RMSE) of predictions of average moisture content by moving and immobilizing boundary methods

Drying condition		R^2		RMSE	
Foam density (g/cm^3)	Drying temperature (°C)	moving	immobilizing	moving	immobilizing
0.3	60	0.98	0.56	0.13	0.63
	70	0.98	0.43	0.14	0.65
	80	0.98	0.49	0.14	0.66
0.5	60	0.99	0.93	0.12	0.28
	70	0.98	0.93	0.14	0.30
	80	0.99	0.90	0.11	0.32
0.7	60	0.98	0.96	0.12	0.19
	70	0.99	0.96	0.12	0.19
	80	0.99	0.96	0.10	0.18